Geological Society, London, Special Publications

The seasonal and vertical distribution of living planktic foraminifera in the NW Arabian Sea

Frank J. C. Peeters and Geert-Jan A. Brummer

Geological Society, London, Special Publications 2002; v. 195; p. 463-497
doi: 10.1144/GSL.SP.2002.195.01.26

The seasonal and vertical distribution of living planktic foraminifera in the NW Arabian Sea

FRANK J. C. PEETERS & GEERT-JAN A. BRUMMER
Department of Marine Chemistry and Geology (MCG), Netherlands Institute for Sea Research (NIOZ), PO Box 59, 1790 Den Burgh, Texel, The Netherlands

Abstract: The NW Arabian Sea is characterized by a strong seasonal contrast in surface water hydrography. During the SW monsoon of 1992, we encountered strong coastal upwelling characterized by low sea surface temperatures (SST), high nutrient concentrations, a shallow thermocline and a near-surface chlorophyll maximum. By contrast, the hydrography during the NE monsoon of 1993 was characterized by a relatively warm nutrient-depleted surface mixed layer and a deep chlorophyll maximum. We show that the faunal composition, depth habitat and abundance of living planktic foraminifera respond to the hydrographic changes controlled by the seasonally reversing monsoon system. Total shell concentrations (>125 μm) ranged from 4 to 332 individuals (ind.) m^{-3} during upwelling and from 3 to 85 ind. m^{-3} during the non-upwelling season. During upwelling, the fauna was dominated by *Globigerina bulloides*. During non-upwelling the fauna was characterized by relatively high concentrations of tropical symbiont-bearing species such as *Globigerinoides ruber*, *Globigerinoides sacculifer* and *Globigerinella siphonifera*, whereas concentrations of *Globigerina bulloides* were an order of magnitude lower. Factor analysis on 15 species yields an upwelling assemblage (UA), a tropical assemblage (TA) and a subsurface assemblage (SA). A fourth factor represents the distribution of the species *Globigerina falconensis*, which is mainly found in subsurface waters during the non-upwelling period (NE monsoon). A model is presented to calculate the base of the productive zone from the vertical shell concentration profile of a given species. The model is validated by comparing the range in calcification temperatures of *G. bulloides*, derived from its $\delta^{18}O$, with the *in situ* sea-water temperature range of the productive zone as predicted from the model. It appears that shell growth (calcite precipitation) is restricted to the productive zone as defined by this method. The average calcification temperature of *G. bulloides* corresponds to the point of maximum change in the shell concentration profile (i.e. the inflection point). For most shallow-dwelling species, the inflection point is found at or below the depth of the chlorophyll maximum, although above the main thermocline. This study indicates that the depth habitat and abundance of different species varies seasonally. Consequently, the abundance and stable isotope composition of specimens in the fossil record reflects a mixture of specimens that were produced at various depths during the different seasons.

In the NW Arabian Sea, coastal upwelling and biological productivity are strongly coupled and mainly controlled by the seasonally reversing monsoon system (Prell & Curry 1981; Anderson & Prell 1991; Prell *et al.* 1992, 1993; Banse 1994; McCreary *et al.* 1996; Rostek *et al.* 1997). The stable isotope composition of planktic foraminiferal shells ($\delta^{13}C$, $\delta^{18}O$) and the abundance of species have been used to reconstruct changes in monsoon history, upwelling intensity, biological productivity and the sea surface temperature of the Arabian Sea (Hutson & Prell 1980; Kroon *et al.* 1990; Prell *et al.* 1992; Anderson & Prell 1991, 1993; Anderson *et al.* 1992; Brock *et al.* 1992; Steens *et al.* 1992; Anderson & Thunell 1993; Naidu & Malmgren 1996*a*, *b*; Rostek *et al.* 1997; Ivanova *et al.* 1999; Ivanova 2000). Paradoxically, much of our knowledge on the environmental preferences of planktic foraminifera has been derived from fossil shells on the ocean floor. The characteristics of the faunal assemblages and the stable isotope composition of individual species were, by analogy, related to characteristics of the present-day upper ocean (Hutson & Prell 1980; Kroon *et al.* 1990; Steens *et al.* 1992; Ivanova 2000). In the sediment, however, the faunal assemblages are mixed by bioturbation and thus may represent a time span from tens to hundreds of years, thus covering many annual cycles.

Investigations on field collected foraminifera have proven to be very useful to characterize the ecology of the species, hence their usage for palaeoenvironmental reconstructions (e.g. Bé & Tolderlund, 1971; Fairbanks & Wiebe 1980; Deuser *et al.* 1981; Kroon & Ganssen 1989;

From: CLIFT, P.D., KROON, D., GAEDICKE, C. & CRAIG, J. (eds) 2002. *The Tectonic and Climatic Evolution of the Arabian Sea Region*. Geological Society, London, Special Publications, **195**, 463–497.

Ravelo *et al.* 1990; Ottens 1992; Ravelo & Fairbanks 1992; Kemle-von Mücke 1994; Watkins *et al.* 1996, 1998; Ufkes *et al.* 1998; Watkins & Mix 1998). In the Arabian Sea, however, the number of systematic studies on living foraminifera is rather limited and often lacks a seasonal coverage. The Arabian Sea region is most interesting for the study of ecology of living planktic foraminifera because of the strong monsoon-controlled seasonal variation in sea surface hydrography.

In this paper we discuss the temporal and spatial distribution of planktic foraminifera in relation to seasonal upwelling in the northwestern Arabian Sea. The seasonal contrast is covered by two sample-sets of depth-stratified plankton tows that were collected along a transect perpendicular to the coast of Yemen–Oman in August 1992 (SW monsoon) and February 1993 (NE monsoon), respectively (Fig. 1). Our objectives are to determine the seasonal and depth distribution of various species, to identify foraminiferal variables that represent a certain state of the ocean and to assess the relationship between the living standing stock and the export flux of foraminiferal shells settling to greater depth.

Material

Sample collection

During the C cruises of R.V. *Tyro* to the Arabian Sea (Van Hinte *et al.* 1995), depth-stratified

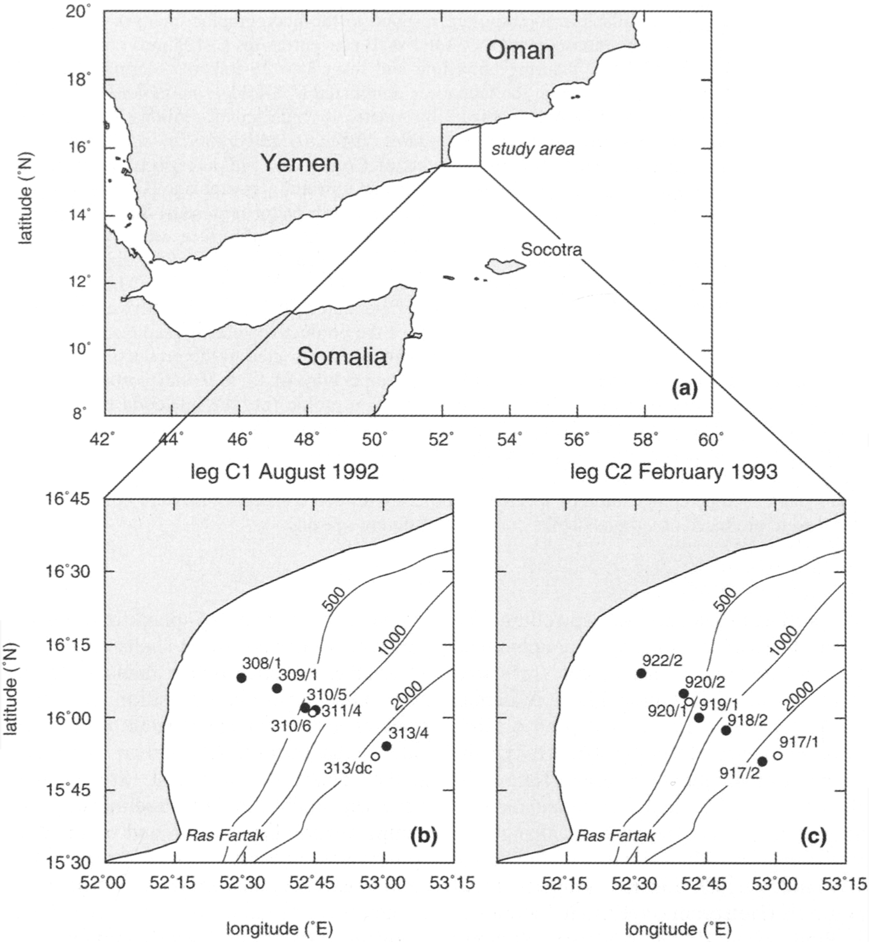

Fig. 1. (**a**) Map showing location of (**b**) and (**c**). (**b**) Map of the Oman–Yemen transect with locations of multinet casts taken during leg C1 of the Netherlands Indian Ocean Program of R.V. *Tyro*, in August 1992. ●, shallow casts (100–0 m); ○, deep casts (500–0 m). Isobaths are given in metres. (**c**) same as (**b**) for leg C2 in February 1993. It should be noted that the same locations have different station numbers; stations 313 and 310 are identical to stations 917 and 920.

plankton tows were collected off the Arabian Peninsula in August 1992 (leg C1) and February 1993 (leg C2) (Fig. 1). The transect was sampled at five stations (Table 1). The upper water column was sampled at five standard depth intervals, 100–75, 75–50, 50–25, 25–10 and 10–0 m. A Hydrobios Multinet system with depth sensor and flow-meter was equipped with five 100 μm plankton nets, which are opened at depth and closed consecutively during the upcast while towed behind the ship. During each leg, an additional deep cast was taken at two stations to a depth of 500 m, covering intervals of 500–300, 300–200, 200–150, 150–100 and 100–0 m. The shallowest net of the deep cast covers the entire shallow cast and has not been studied. To avoid clogging of the net, varying amounts of water were filtered depending on the expected amount of particulate matter. For the deep cast characteristically 100–500 m^3 were filtered per interval, and for shallow casts generally 20–100 m^3 per interval. Samples were stored in a borax-buffered formalin–sea-water solution (pH >8.0), in 500 ml LDPE bottles, kept under dark and cool conditions and checked for their pH. Further details have been given by Brummer (1995).

Conductivity–temperature–depth (CTD) profiles

To compare the faunal distribution patterns and depth habitat of living planktic foraminifera with water column properties, 11 CTD-rosette casts were taken along the transect (Figs. 2 and 3, Table 2). The following selection of variables is used in this study: temperature, salinity, density, fluorescence and nitrate concentration. Technical procedures and calibration of the data have been given by Van Hinte *et al.* (1995). On the basis of the temperature profile the upper water column is subdivided into the surface mixed layer, the upper thermocline and the lower thermocline. In this study the depth of the surface mixed layer is found at SST − 0.5 °C, whereas the depth of the thermocline is defined as the largest minimum in the first derivative of temperature with depth.

Sample preparation

In the laboratory, the plankton tow samples were split into eight aliquots using a Fritsch Laborette 27 Rotary Cone Sample Divider. Six aliquots (three-quarters of the total sample) were used for foraminiferal analysis and one aliquot for chemical analysis (not discussed herein). The remaining aliquot is stored in a sea-water solution with a pH of 8.0–8.5 and kept under cool and dark conditions. The sample aliquots for foraminiferal analysis were frozen in liquid nitrogen using preweighed aluminium cups, freeze-dried, stored in an desiccator with silica gel for at least 3 h and weighed on a Sartorius Analytic balance with a precision of ±0.1 mg. The dry weight of this residue, representing the total biomass between 100 and 1000 μm (Table 1; Figs. 2f and 3f), is weighed at 30 s intervals over a period of 3 min to correct for moisture uptake. The organic matter was removed using a low-temperature asher. The ashed residue was wet sieved over mesh sizes of 500, 355, 250, 150 and 125 μm and rinsed with ethanol (Peeters *et al.* 1999). The separate size fractions were dried on a hot plate at 80°C for *c.* 30 min and analysed for their foraminiferal composition. At least 200 specimens per fraction were counted. If fewer than 200 specimens were present, which was the case in most of the larger fractions, the entire fraction was counted. Total standing stock (individuals (ind.) m^{-3}) and planktic foraminiferal census counts are given in Appendices A and B. The average size of foraminiferal shells (>125 μm) is calculated using a weighted averaged mean of number of shells per size fraction following the method discussed by Peeters *et al.* (1999). In total, 64 samples have been used in this study. Planktic foraminifera were identified using a WILD M5A binocular microscope following the taxonomy of Bé (1967) and Hemleben *et al.* (1989).

Stable isotope analysis

Whole shells of *G. bulloides* were hand picked from the size fractions 150–250 and 250–355 μm. The stable isotope composition of the shells was measured on a Finnigan 251 gas source mass spectrometer equipped with an automated carbonate extraction line. All analyses were carried out at the Faculty of Earth and Life Sciences at the Vrije Universiteit in Amsterdam, The Netherlands. Samples were dissolved in concentrated orthophosphoric acid at 80 °C. Approximately 30–80 μg of sample was used per analysis. Results are reported in the conventional δ-notation as per mil deviation from the Vienna-Pee Dee Belemnite standard (V-PDB). Calibration to the V-PDB standard was performed via NBS-18, NBS-19 and NBS-20 international standards (Coplen *et al.* 1983; Hut 1987). The external reproducibility for $\delta^{18}O$ is ±0.08‰ and for $\delta^{13}C$ is ±0.04‰.

Table 1. *Location and sample details of multi-net stations 308–313 of the C1 cruise in August 1992, and of stations 917–922 of the C2 cruise in February 1993*

Station-cast-net	Date, local time	Decimal longitude (°N)	Decimal latitude (°E)	Distance from coast (km)	Depth start (m)	Depth end (m)	Volume filtered (m^3)	Biomass (mg m^{-3})
308-1-5	19 Aug. 1992, 09:25	52.50	16.14	30.28	22.8	0.0	103	51.7
308-1-4					47.5	22.8	55	13.2
308-1-3					72.1	47.5	48	8.0
308-1-2					98.1	72.1	66	3.2
309-1-5	19 Aug. 1992, 17:31	52.64	16.09	45.84	8.0	0.0	36	60.5
309-1-4					18.2	8.0	26	25.9
309-1-3					28.3	18.2	25	17.8
309-1-2					49.5	28.3	42	11.7
310-5-5	20 Aug. 1992, 15:37	52.73	16.02	59.12	8.1	0.0	41	62.9
310-5-4					23.3	8.1	34	23.9
310-5-3					48.5	23.3	44	12.7
310-5-2					74.3	48.5	40	5.4
310-5-1					99.6	74.3	33	4.2
310-6-4	20 Aug. 1992, 17:08	52.75	16.00	61.72	148.1	97.6	35	6.5
310-6-3					200.2	148.1	53	4.9
310-6-2					298.3	200.2	104	4.9
310-6-1					498.4	298.3	270	2.9
311-1-5	21 Aug. 1992, 09:50	52.75	16.00	61.42	7.6	0.0	52	60.2
311-1-4					23.3	8.1	50	29.1
311-1-3					49.5	23.3	132	11.4
311-1-2					73.8	49.5	124	7.3
311-1-1					96.1	74.8	36	4.2
313-4-5	21 Aug. 1992, 12:20	53.02	15.91	93.42	8.1	0.0	25	259.9
313-4-4					24.3	10.1	41	171.9
313-4-3					48.5	24.3	87	34.8
313-4-2					73.8	49.5	87	18.8
313-4-1					99.6	74.8	60	9.3
313-dc-4	22 Aug. 1992, 12:10	52.94	15.88	86.43	147.6	99.1	94	6.2
313-dc-3					196.1	149.6	98	9.8
313-dc-2					300.3	199.2	278	14.2

313-dc-1					498.0	300.3	478	10.9
917-2-5	25 Feb. 1993, 09:15	52.92	15.90	83.68	12.1	0.0	21	40.7
917-2-4					27.3	12.1	22	66.2
917-2-3					51.6	27.3	43	80.8
917-2-2					77.9	51.6	79	19.6
917-2-1					102.1	77.9	68	12.1
917-1-4	25 Feb. 1993, 08:15	52.97	15.89	88.71	153.0	101.0	75	10.1
917-1-3					203.0	153.0	75	10.7
917-1-2					302.0	203.0	184	2.8
917-1-1					502.0	302.0	240	6.6
918-2-5	26 Feb. 1993, 09:40	52.84	15.96	72.74	12.1	0.0	35	43.2
918-2-4					27.3	12.1	47	71.1
918-2-3					51.6	27.3	97	76.1
918-2-2					77.9	51.6	132	23.9
918-2-1					103.1	77.9	101	14.1
919-1-5	26 Feb. 1993, 16:47	52.73	16.00	58.99	10.1	0.0	12	61.0
919-1-4					26.3	10.1	19	22.3
919-1-3					51.6	26.3	50	89.4
919-1-2					76.8	51.6	91	23.6
919-1-1					102.1	76.8	70	9.5
920-2-5	27 Feb. 1993, 09:15	52.64	16.08	47.08	11.1	0.0	16	54.0
920-2-4					27.3	11.1	46	36.3
920-2-3					52.6	27.3	79	52.1
920-2-2					77.9	52.6	135	15.9
920-2-1					102.1	77.9	105	12.2
920-1-4	27 Feb. 1993, 08:15	52.70	16.09	52.53	153.0	103.0	168	7.0
920-1-3					202.0	153.0	146	7.7
920-1-2					303.0	202.0	269	27.9
920-1-1					501.0	303.0	282	15.1
922-2-5	27 Feb. 1993, 08:00	52.52	16.17	30.99	12.1	0.0	48	77.2
922-2-4					26.3	12.1	58	67.2
922-2-3					51.6	26.3	106	45.7
922-2-2					77.0	51.6	149	16.3
922-2-1					102.1	77.0	169	4.7

Biomass represents the dry weight of particulate matter between 100 and 1000 μm. ‘Swimmers’ were excluded from these measurements.

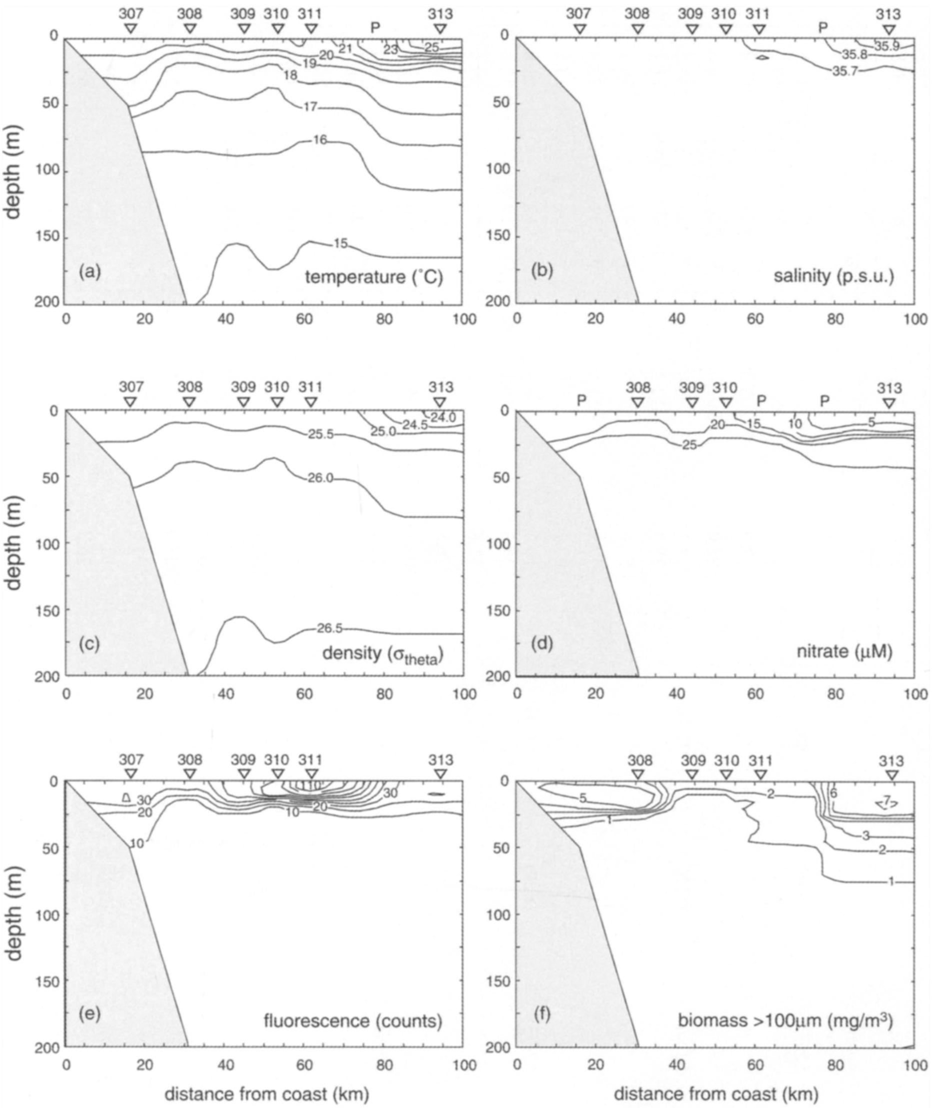

Fig. 2. (**a**) Temperature, (**b**) salinity, (**c**) density, (**d**) nitrate concentration, (**e**) fluorescence and (**f**) biomass distribution along the Oman–Yemen transect in August 1992 (SW monsoon season). At stations 308–311, cold and nutrient-rich water is found near the sea surface, indicating freshly upwelled waters. At the end of the transect (station 313), a relatively warm-water eddy is encountered, as indicated by a higher temperature and salinity and lower nitrate concentrations near the sea surface. It should be noted that fluorescence (chlorophyll) maxima are found near the sea surface. At top of figures: triangles indicate, station numbers; P, surface water observation from 3 m water depth, either from aqua-flow system or plankton pump sample.

Methods

Contouring data

To assess the spatial distribution pattern of foraminifera, CTD data and $\log_4$ transformed species concentrations were plotted and computer contoured using an inverse distance squared variable radius search algorithm (Figs 2 and 3; see also Figs 5 and 6). Because the largest changes in the distribution (absolute abundance) pattern of planktic foraminifera occur in the upper part of the water column, contour plots and shell concentration profiles are drawn for the upper 200 m.

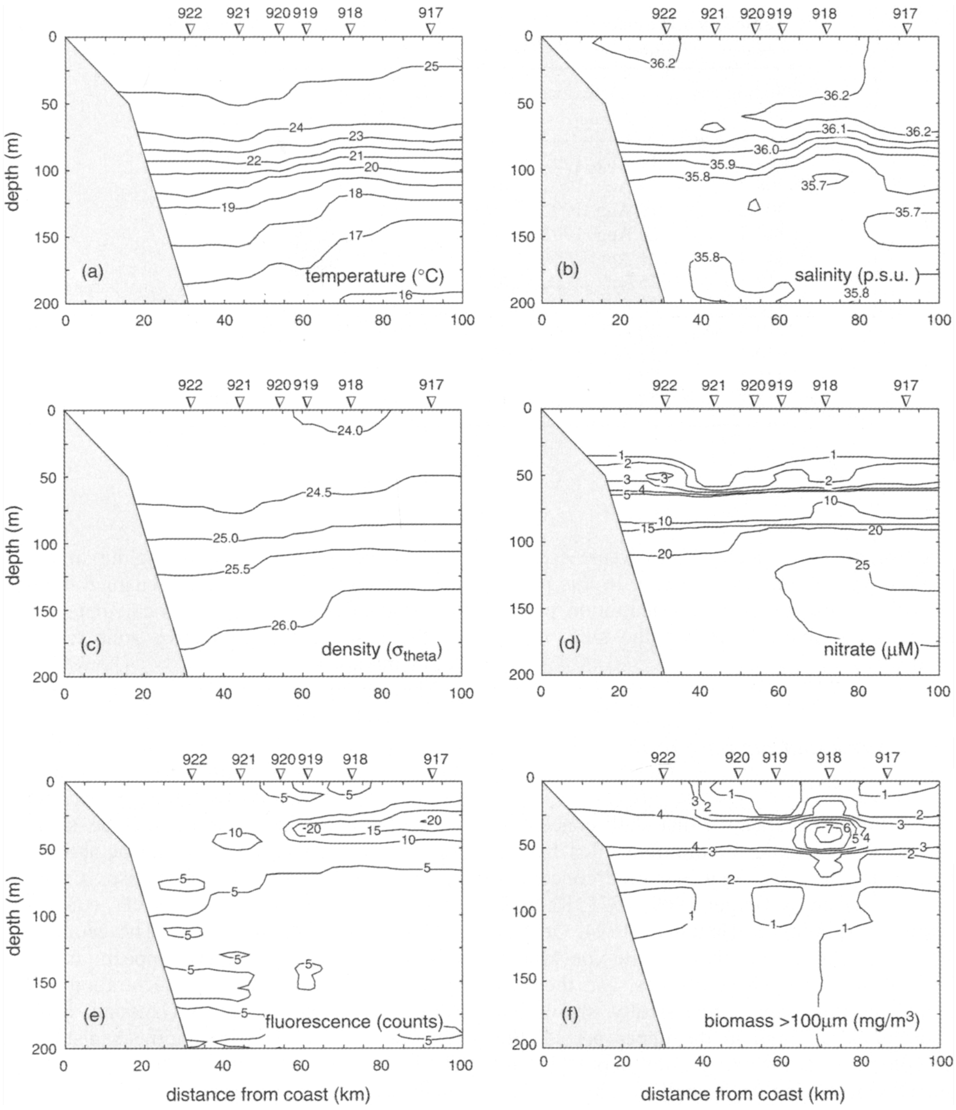

Fig. 3. (**a**) Temperature, (**b**) salinity, (**c**) density, (**d**) nitrate concentration, (**e**) fluorescence and (**f**) biomass distribution in February 1993 (NE monsoon season). A warm and oligotrophic uniform surface layer characterizes the transect in winter. A deep fluorescence (chlorophyll) maximum is found at *c*. 40 m and the main thermocline at *c*. 100 m.

Dead or alive?

Living and dead specimens in plankton nets may be distinguished by the presence or absence of cytoplasm and sometimes by its colour (e.g. Berger 1971; Hemleben *et al.* 1989; Kemle-von Mücke 1994; Ortiz *et al.* 1995; Schiebel *et al.* 1995). Separating living from dead specimens in this way is time consuming and not very precise considering the slow cytoplasm decomposition after death, during the descent to the sea floor. Often, plasma-filled tests of foraminifera are found far below the zone in which shell growth (productive zone) takes place (Schiebel *et al.* 1995). By contrast, empty tests have been found within the zone where production takes place (Berger 1971; Schiebel *et al.* 1995). The presence/absence of colour of the cytoplasm therefore does not allow identification of the exact position between the productive zone and the settling flux zone below, i.e. the base of the productive zone

Table 2. *Locality details of CTD stations taken during C cruises leg 1 (August 1992) and leg 2 (February 1993)*

Station-cast	Date, local time	Dec. longitude (°N)	Dec. latitude (°E)
307-1	19 Aug. 1992, 6:15	52.38	16.18
308-2	19 Aug. 1992, 9:40	52.52	16.13
309-2	19 Aug. 1992, 18:21	52.63	16.10
310-1	20 Aug. 1992, 11:35	52.70	16.07
313-4	21 Aug 1992, 14:47	53.00	15.88
917-1	25 Feb. 1993, 12:02	53.00	15.87
918-1	25 Feb. 1993, 19:15	52.83	15.98
919-1	26 Feb. 1993, 15:44	52.75	16.02
920-1	27 Feb. 1993, 10:40	52.70	16.07
921-1	27 Feb. 1993, 17:32	52.60	16.07
922-1	28 Feb. 1993, 8:31	52.53	16.18

(Z_{BPZ}). Consequently, one needs to define Z_{BPZ} for the various species on other criteria. In this paper, we propose to use the shell concentration profile to define Z_{BPZ} and to estimate the size of the standing stock.

Standing stock and the base of the productive zone

Previous studies have shown that shell concentration profiles of planktic foraminifera often have a characteristic shape (see, e.g. the shell concentration profiles given by Berger 1969, 1971; Kahn & Williams 1981; Bijma & Hemleben 1994; Ortiz *et al.* 1995; Schiebel *et al.* 1995; Kemle-von Mücke & Oberhänsli 1999). These profiles, and the data presented in this paper, consistently show that shell densities are high in the upper part of the water column and low at greater depths in the ocean. Obviously, the high shell densities in the upper part of the water column mostly represent specimens that are alive and capable of adjusting their buoyancy by producing low-density lipids or gases to counter gravitational settling (Furbish & Arnold 1997). At greater depth in the water column, the shell densities are low and relatively constant. Specimens found in this part of the water column represent the 'pelagic rain' of exported shells that settle to the sea floor. We propose to use the shape of the shell concentration profile to identify a depth level that separates the water column into two zones: (1) the productive zone (PZ), in which most specimens are alive and precipitate their primary calcite; (2) the settling flux zone (SFZ), in which the specimens mostly represent the exported shells that settle to the sea floor. The boundary between the PZ and the SFZ is characterized by a rapid decline in the shell concentration with depth and is named the base of the productive zone (Z_{BPZ}). To calculate the depth of the base of the productive zone we use the following approach.

The SFZ is characterized by a constant and relatively low shell concentration, which we will call C_{SF}. The depth at which the concentration of shells approximately equals C_{SF} is considered as the base of the productive zone. In practice, the base of the productive zone will be somewhere within a tow interval and cannot be assigned to a specific depth. We therefore use a curve fit procedure to describe the shell concentration profile by a continuous curve. The geometry of a Gaussian distribution curve appears to be very similar to most shell concentration profiles. Although we realize that a Gaussian distribution function does not describe the mechanistic process of shell production and the loss of foraminifer shells as a result of grazing and mortality and subsequent settling, it does describe the most important phenomena that are frequently observed in the concentration profiles of different species. In Fig. 4, for example, we show that the maximum in the shell concentration profile is described by the maximum of the Gaussian curve, whereas the lower shell concentrations that are found at greater depths in the ocean are fitted by the 'tail' of the curve. Obviously, modelling the characteristics of the shell concentration profile of a given species is very informative and permits a detailed comparison of the vertical distribution of living planktic foraminifera to hydrographic features (e.g. mixed-layer depth, thermocline depth or depth of chlorophyll maximum). It also may be used to extract environmental information from the living planktic foraminifera that can be used for the reconstruction of SST, thermocline depth, biological productivity, mixed-layer depth, etc. (e.g. Ravelo & Fairbanks 1992; Watkins & Mix, 1998).

Collecting foraminifera using depth-stratified tows results in a total number of foraminifera caught per depth interval, N_i (number of specimens). The concentration of foraminifera per unit volume of water, C_i (ind. m^{-3}), is calculated using

$$C_i = \frac{N_i}{V_i} \qquad (1)$$

in which V_i (m^3) is the volume of sea water filtered per net as measured by a flow meter. It can be expected that most of the specimens caught in the upper part of the water column are alive (e.g. Berger 1969), whereas deeper in the water column an increasing proportion of dead specimens is found. The total concentration of specimens as a function of depth ($C(z)$) is given by the sum of living ($C_L(z)$) and dead specimens ($C_D(z)$), so that

$$C(z) = C_L(z) + C_D(z). \qquad (2)$$

Below the base of the productive zone, we must assume that specimens are dead, and that their concentration remains approximately constant and equals C_{SF}:

$$C(z) = C_D(z) = C_{SF} \quad (\text{for} \quad z > z_{BPZ}). \qquad (3)$$

With z representing the depth of the water column in metres. The concentration of dead specimens at any depth above z_{BPZ} is assumed to linearly increase with depth from zero at the sea surface to a value of C_{SF} at the base of the productive zone (Fig. 4). The concentration of dead specimens at any depth above Z_{BPZ} is thus given by

$$C_D(z) = C_{SF}\frac{z}{z_{BPZ}} \quad (\text{for} \quad z \leq z_{BPZ}). \qquad (4)$$

To fit the concentration profile of living specimens, $C_L(z)$, we use a Gaussian distribution:

$$C_L(z) = \frac{a}{\sigma\sqrt{2\pi}}\exp\left[-0.5\left(\frac{z-c}{\sigma}\right)^2\right] \qquad (5)$$

in which a, c and σ are parameters related to the total area under the curve, the centre of distribution and standard deviation, respectively (Fig. 4). Consequently, the total concentration as a function of depth, including both living and dead specimens, is described by the sum of equations (4) and (5), yielding

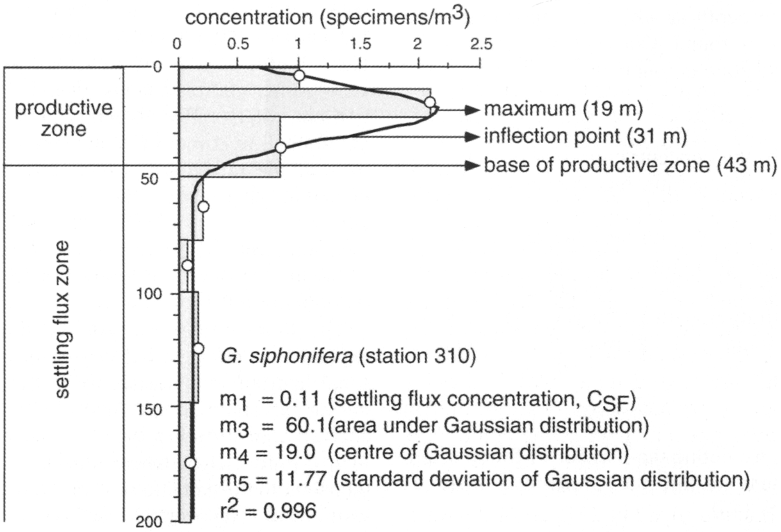

Fig. 4. Schematic representation of the vertical distribution of *Globigerinella siphonifera* at station 310 (upwelling station during the SW monsoon season, August 1992), illustrating position of concentration maximum, inflection point and the base of the productive zone. Parameter m_1 reflects the export flux shell concentration (C_{SF}) and is assumed to be constant (i.e. the shell concentration below the productive zone). The inflection point, representing the point of maximum change of the concentration with depth, is found by adding one standard deviation (m_5) to the depth at which the maximum concentration (m_4) is found, which in this case equals 30.8 m (i.e. 19.0 m + 11.8 m). The base of the productive zone is defined at two standard deviations below the depth at which the maximum is found ($m_4 + 2m_5$). Parameter m_3 represents the total area under the total Gaussian distribution, and can be used in standing stock calculations. It should be noted that m_3 does not represent the standing stock, as it needs to be corrected for that part of the curve that is present between the sea surface and the base of the productive zone. (For further explanation, see text.)

$$C(z) = C_{\mathrm{SF}}\frac{z}{z_{\mathrm{bpz}}} + \frac{a}{\sigma\sqrt{2\pi}}\exp\left[-0.5\left(\frac{z-c}{\sigma}\right)^2\right] \quad (\text{for} \quad z \leq z_{\mathrm{BPZ}}). \quad (6)$$

If two maxima are present in the shell concentration profile (see, for example, the shell concentration profile of *G. menardii* at station 310 in Fig. 8, below), we use an additional Gaussian distribution to fit the data. In such cases the parameters of the first and second distribution are numbered (e.g. the centres of the first and second Gaussian distribution are named c_1 and c_2, respectively). The depth at which the total shell concentration $C(z)$ approaches C_{SF} must be defined as the base of the productive zone. However, one might argue about the criteria that should be used to place this boundary. We must therefore find a practical measure to identify the base of the productive zone; that is, a depth level that separates the majority of the living specimens in the surface layers from a zone below that is dominated by dead specimens. Assuming that living specimens in the water column are described by the Gaussian distribution function of equation (5), one might expect that about 95% of the living population is present within two times the standard deviation (SD) from the centre of the distribution; that is, 2 SD below the depth at which the maximum shell concentration is found. Consequently, the base of the productive zone is found at

$$z_{\mathrm{BPZ}} = c + 2\sigma. \quad (7)$$

At this depth, the concentration of shells approximately equals the settling flux concentration (Fig. 4) and: $C(z_{\mathrm{BPZ}}) \approx C_{\mathrm{SF}}$. If the shell concentration profile shows a maximum near the sea surface (in the uppermost plankton net), then $c = 0\mathrm{m}$. It should be noted that the maximum change of the shell concentration with depth (i.e. the inflection point, z_{I}) is found at 1 SD from the maximum of the Gaussian curve:

$$z_{\mathrm{i}} = c + \sigma. \quad (8)$$

In this paper we define the number of foraminifera that is present within the productive zone as standing stock (*SS*):

$$SS = \int_{z_0}^{z_{\mathrm{B}}} C(z) \quad \mathrm{d}z. \quad (9)$$

However, because a small part of the specimens above z_{BPZ} will be dead and should not be included in the standing stock estimates, we also define the corrected standing stock (SS_{COR}), by subtracting the concentration of dead specimens from the total concentration:

$$SS_{\mathrm{COR}} = \int_{z_0}^{z_{\mathrm{B}}} C_{\mathrm{L}}(z) \quad \mathrm{d}z = \int_{z_0}^{z_{\mathrm{B}}} [C(z) - C_{\mathrm{D}}(z)] \quad \mathrm{d}z \quad (10)$$

which thus represents the expected number of living specimens (ind. m^{-2}) found in the productive zone; that is, in a vertical section of the water column ranging from the sea surface to z_{BPZ}. In practice, the number of dead specimens in the productive zone appears to be very small compared with the number of living specimens, so that $SS \approx SS_{\mathrm{COR}}$.

Results

Hydrographic conditions

During leg C1, in August 1992 (SW monsoon), the Oman transect was characterized by coastal upwelling (Figs 1 and 2). Near the coast, surface water temperatures (at 5 m) were low (20.5 °C) and nitrate concentrations at the surface were high (17.2–18.5 μM) (Fig. 2a and d). At the offshore end of the transect (at station 313), we encountered a warm mesoscale eddy with a surface temperature of 25.7 °C and 2.5 μM of nitrate. Depth profiles indicate a shallow surface mixed layer depth of *c.* 10 m at all stations.

In contrast, hydrographic conditions during the leg C2 cruise in February 1993 (NE monsoon) were rather uniform (Figs 1 and 3). Along the transect, SST varied around 26 °C and a deep chlorophyll maximum (DCM), associated with the base of the mixed layer, had developed at about 40–50 m (Fig. 3e). The main thermocline is situated at about 100 m. Surface water nutrient concentrations were two orders of magnitude lower than measured during the SW monsoon (Brummer 1995).

The hydrography, as sampled during the two expeditions, characteristically represents the seasonal hydrographic variability in this area, in that during the summer SW monsoon cold and nutrient-rich water reaches the surface, enhancing biological productivity, whereas during the winter NE monsoon the ocean stratifies and a relatively thick, warm and oligotrophic surface layer develops. Consequently, the hydrography during leg C1 and leg C2 may be considered as hydrographic end-members.

Fauna composition and species distribution patterns

In total, 26 species of planktic foraminifera (>125 μm) are identified in the 64 plankton net samples (Appendices A and B). The 10 most abundant species (Table 3) account for more than 95% of the fauna. The concentration of foraminifera (>125 μm) in the water column ranges from 4 to 332 ind. m^{-3} in August 1992 during upwelling and from 3 to 85 ind. m^{-3} in February 1993 when no upwelling occurred. Contour plots of $\log_4$ transformed shell concentrations of the 15 most abundant species >125 μm are given in Figs. 5 and 6. It should be noted that we use a $\log_4$ transformation on the shell concentrations only for the purpose of contouring. This transformation results in contour intervals that appeared to be most practical for visualization of the data.

A factor analysis with Varimax Rotation using SYSTAT was performed on 15 species, using all 64 plankton tows. The remaining 11 species, with a per cent abundance of lower than 0.4%, had low squared multiple correlation with all other variables and were removed from the original data before analysis (Tables 3 and 4). To increase normality of the data (Tabachnick & Fidell 1996), the species concentrations were $\log_e$ transformed. In case a species was absent in a sample, the sample is excluded from the analysis (i.e. pairwise deletion). Considering only eigenvectors greater than 1.0, there appear to be four important factors, which together explain 85% of the total variance (Table 4). Species factor scores are given in Table 4 and represent correlations between species (variables) and factors. The higher the score, the better the species is a pure measure of the factor.

Table 3. *Per cent abundance of planktic foraminifera (>125 μm) for leg 1 (August 1992) and leg 2 (February 1993) samples, as well as for the total dataset*

Species	% in C1 dataset	% in C2 dataset	% in total dataset
G. bulloides	62.04	4.25	43.22
G. ruber	2.51	26.63	10.37
G. glutinata	8.99	11.98	9.96
G. calida	10.37	8.35	9.71
G. siphonifera	1.63	16.74	6.55
G. sacculifer	0.54	16.87	5.86
N. dutertrei	3.55	2.61	3.25
G. tenellus	0.63	6.85	2.65
G. menardii	2.45	1.64	2.18
T. quinqueloba	1.89	0.03	1.29
P.F. indet.	0.67	1.12	0.82
N. pachyderma (sin)	1.19	0.01	0.80
G. falconensis	0.35	1.46	0.71
H. parapelagica	0.63	0.32	0.53
P.F. aberrant	0.66	0.13	0.49
D. anfracta	0.68	0.06	0.48
T. iota	0.63	0.01	0.43
G. uvula	0.24	0.02	0.17
G. hexagona	0.10	0.27	0.15
O. universa	0.01	0.38	0.13
G. scitula	0.15	0.03	0.11
B. digitata	0.02	0.15	0.06
P. obliquiloculata	0.05	0.06	0.05
G. theyeri	0.03	0.01	0.02
G. rubescens	0.00	0.01	0.00
G. tumida	0.00	0.00	0.00
G. adamsi	0.00	0.00	0.00
T. humilis	0.00	0.00	0.00

Factor 1: the upwelling assemblage (UA, explaining 29.6% of total variance). Species that show high scores on the first factor are *D. anfracta*, *N. pachyderma* (sin), *T. quinqueloba*, *G. bulloides*, *N. dutertrei* and *G. menardii*. Highest shell concentrations of these species are mostly found during upwelling as sampled during leg C1 (Figs 5 and 6). According to Bé & Tolderlund (1971), the species in the upwelling assemblage have their maximum occurrence in different faunal provinces: *N. pachyderma* (sin) in the polar province, *G. bulloides* and *T. quiqueloba* in the subtropical province, *N. dutertrei* in the transitional to subtropical provice and *G. menardii* in the subtropical to tropical provice. *D. anfracta* is probably restricted to transitional–temperate to tropical provinces. Because of its small adult size it is routinely underrepresented in conventional collections >150 μm (Brummer & Kroon 1988; Peeters *et al.* 1999). Despite their maximum abundance in different faunal provinces, the concomitant occurrence of these species indicates high nutrient availability. Judging from the factor pattern, two sub-assemblages may be recognized within the upwelling assemblage.

(1) Upwelling assemblage-A (UA-A). The scores of *G. bulloides*, *N. dutertrei* and *G. menardii*on the first factor are slightly lower than those of the other species involved and may show an increased score on the second and/or third factor to account for presence during non-upwelling (Factor 2, *N. dutertrei*) or suggesting a deeper habitat (*G. menardii*). Although more abundant during upwelling than during non-upwelling, these species are consistently present during both monsoon seasons. It is suggested that they reflect fertile regions in a more general sense; that is, as also observed in central parts of the Arabian Sea (Curry *et al.* 1992).

(2) Upwelling assemblage-B (UA-B). *D. anfracta*, *N. pachyderma* (sin) and *T. quinqueloba* have highest positive scores only on Factor 1. These (small) species were abundant only during upwelling, and were virtually absent during the non-upwelling period. As *N. pachyderma* (sin) and *T. quinqueloba*are known to represent cold waters at higher latitudes (Bé & Tolderlund, 1971), these species may be close to their upper thermal

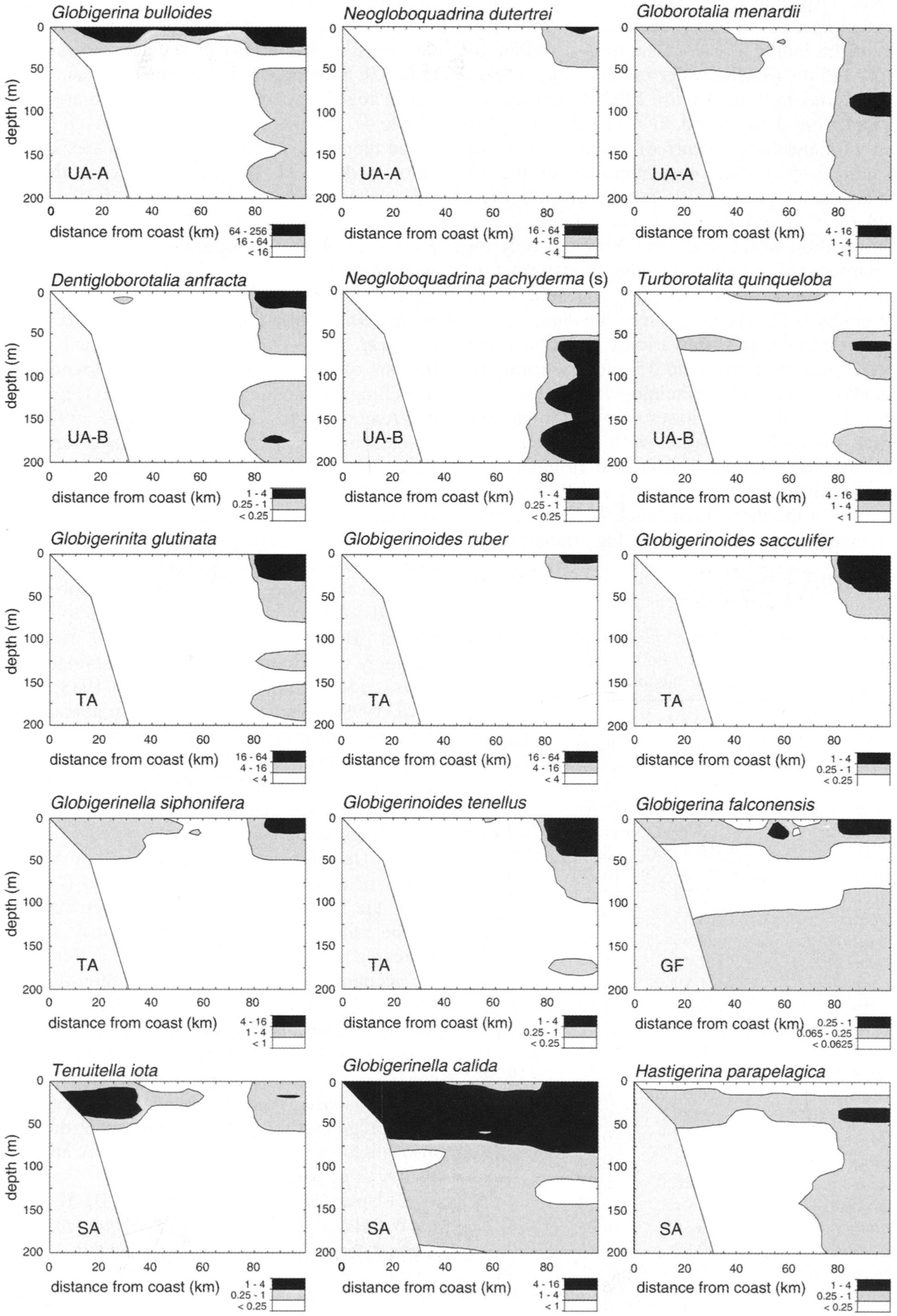

Fig. 5. Contoured distribution patterns of the most abundant species of planktic foraminifera during the SW monsoon leg 1 survey in August 1992. It should be noted that the shell concentrations have been $\log_4$ transformed and that the contour intervals are adjusted to the maximum concentration.

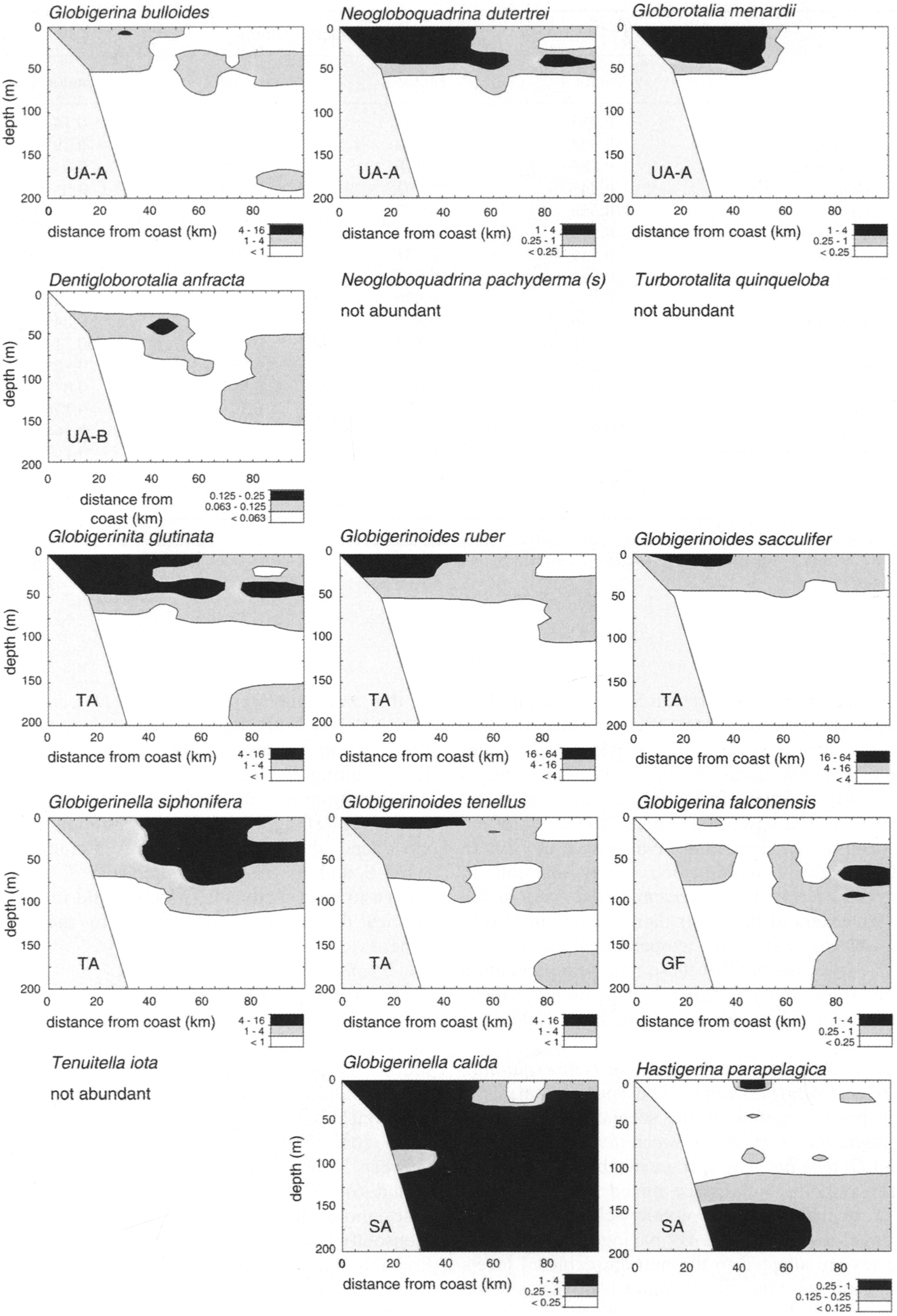

Fig. 6. Contoured distribution patterns of the most abundant species of foraminifera during the NE monsoon leg 2 survey in February 1993. It should be noted that the shell concentrations of the species have been $\log_4$ transformed and that the contour intervals are adjusted to the maximum concentration.

Table 4. *Factor scores of $\log_e$ transformed species concentrations*

	Rotated factor pattern			
	Factor 1	Factor 2	Factor 3	Factor 4
D. anfracta	**0.933**	0.141	0.258	−0.143
N. pachyderma (sin)	**0.903**	0.170	−0.258	0.299
T. quinqueloba	**0.885**	−0.179	0.248	−0.034
G. bulloides	**0.845**	−0.191	0.464	0.059
N. dutertrei	**0.656**	0.422	0.479	−0.016
G. menardii	**0.562**	0.052	0.418	0.009
G. glutinata	0.559	**0.731**	−0.002	0.157
G. ruber	0.044	**0.965**	−0.081	0.247
G. sacculifer	−0.014	**0.898**	0.107	−0.245
G. siphonifera	−0.036	**0.871**	0.272	0.047
G. tenellus	−0.021	**0.860**	0.037	0.314
T. iota	0.346	0.157	**0.907**	0.181
G. calida	0.047	−0.036	**0.801**	0.072
H. parapelagica	0.273	0.204	**0.576**	−0.176
G. falconensis	0.052	0.239	0.100	**0.964**
% of total variance explained	29.6	28.0	18.1	9.1
Cumulative % of total variance explained	29.6	57.6	75.7	84.7

All 64 plankton tow samples were used for the analysis. Three assemblages are found (see text for discussion). The fourth factor reflects the distribution pattern of *G. falconensis*, explaining an additional 9.1% of the total variance. Bold indicates highest score for each species.

tolerance limit in the Arabian Sea, explaining their deeper habitat and absence during non-upwelling (Figs. 5 and 6). Upwelling of deep cold water during the SW monsoon will bring these species into surface waters indicating the areas of most intense coastal upwelling (Thiede 1975; Giraudeau raudeau & Rogers 1994; Ivanova *et al.* 1999). Interestingly, *T. quinqueloba* occurs not only in the assemblage with *N. pachyderma* (sin) in the colder waters of the lower thermocline but also in the surface waters at temperatures as high as 21 °C. It is possible that these may be a population of the warm-water *T. quinqueloba*, similar to those found in the Coral Sea by Darling *et al.* (2000).

Factor 2: the tropical assemblage (TA, explaining 28.0% of total variance). The species that show high positive scores on the second factor include *G. glutinata*, *G. ruber*, *G. sacculifer*, *G. siphoniferaand* *G. tenellus*. The species inhabit the relatively warm oligotrophic surface mixed layer and were most abundant in the non-upwelling period as sampled during leg C2. By having symbionts, the species are adapted to the nutrient-depleted levels of the photic zone. *G. glutinata* also shows some affinity with the upwelling assemblage.

Factor 3: the subsurface assemblage (SA, explaining 18.1% of total variance). The species present in this assemblage are *G. calida, H. parapelagicaand T. iota*. Although highest concentrations are found during upwelling, these species are also found during the non-upwelling period. Highest concentrations are mostly found in the subsurface. During upwelling, the shell concentration maxima are found shallower than during non-upwelling (Figs 5 and 6). *H. parapelagicaand T. iota* are known to bear symbionts, which would imply that species distributions are limited to the photic zone.

Factor 4: Globigerina falconensis (GF, explaining 9.1% of total variance). The distribution pattern of *G. falconensis* accounts for the presence of a fourth factor. The species inhabits subsurface waters and, in contrast to the SA species, is most abundant during non-upwelling conditions. Maximum concentrations of this species are found between 50 and 100 m, i.e. below the DCM (Figs 5 and 6). *G. falconensis* is approximately four times more abundant during non-upwelling (NE monsoon) than during upwelling (SW monsoon). Probably, this species is the best faunal indicator for NE monsoon conditions. Its relative abundance in the surface sediments of the Arabian Sea increases towards the NE, indicating a stronger influence of NE monsoon conditions (see also Schulz *et al.* 2002).

Depth habitat and hydrography

In this section the depth habitat of various species will be discussed in relation to the hydrography. First we will discuss the results on the two 'upwelling stations', 310 and 313, followed by the 'non-upwelling stations' 920 and 917. Only species with a minimum concentration of 1 ind. m^{-3} in at least one of the nine plankton nets of a given station will be discussed.

Station 310 was located in the centre of upwelling during the SW monsoon of August 1992, characterized by low SST and high nitrate concentrations, indicating freshly upwelled waters (Figs 2 and 7). *G. bulloides* is the most abundant species at this station and inhabits the uppermost part of the water column. The base of the productive zone is found at 17 m. Its inflection point (z_i), which indicates the point of maximum change of the shell concentration with depth, is found at 8 m and coincides with the thermocline and the chlorophyll maximum. *G. glutinata* and *N. dutertrei* show a similar concentration profile: a maximum shell concentration at the sea surface and a shallow base of the productive zone at 21 m and 26 m, respectively. *G. siphonifera* and *G. calida,* however, have subsurface maxima, with the base of their productive zone at 43 m and 41 m, respectively. The latter species thus reflect waters from slightly below the main thermocline. The inflection point of these species appears to coincide with a second, although less pronounced thermocline at a depth of 30 m. The concentration profile of *G. menardii* shows two maxima: a shallow maximum at 17 m and a deeper maximum at 65 m. At this station, the average test size of *G. menardii* increases to a depth of about 85 m (Fig. 8). The shallow maximum apparently represents small or immature specimens, whereas the deeper maximum is associated with relatively large mature specimens. The base of the productive zone is therefore situated below the deepest maximum, close to where *G. menardii* reaches its maximum test size (Fig. 8). This observation confirms that the base of the productive zone indeed reflects the maximum depth at which *G. menardii* lives. The decreasing average test size below the productive zone may be explained by the fact that the specimens are dead, and have lost their ability to counter gravitational settling. The average test size decreases here, because larger shells will settle to the sea floor faster than smaller ones.

Station 313 was located in the core of a relatively warm-water eddy during the SW monsoon of August 1992 (Figs 2 and 9). The chlorophyll maximum, mixed layer and thermocline at this station were all present at a depth of 8–12 m. Lower nitrate concentrations and higher temperature of the surface mixed layer indicate more 'aged' upwelled waters than recorded at station 310 (centre of upwelling). Shell concentrations are generally high, and species show a shell concentration maximum at or near the sea surface, except for *G. calida* and *G. menardii*. The inflection point of *G. bulloides* is found at 12 m and coincides with the thermocline and chlorophyll maximum. The base of its productive zone is found at 23 m. Again, the concentration profile of *G. glutinata* and *N. dutertrei* is similar to that of *G. bulloides*. However, the base of their productive zone is found slightly deeper, at 43 m and 38 m, respectively. Species from the tropical assemblage (TA) (i.e. *G. ruber*, *G. sacculifer*, *G. siphonifera* and *G. tenellus*) are abundant as well at this station, possibly because of the presence of a thin but relatively warm and nutrient-depleted mixed layer. Concentration maxima of these species were found at, or slightly below, the sea surface, whereas inflection points coincide with, or are found just below, the thermocline.

The base of the productive zone of these species varies between 25 m (*G. ruber*) and 51 m (*G. siphonifera*). *G. calida* and *G. menardii* show a subsurface maximum with a slight increase of the concentration near the sea surface. Again, the base of the productive zone is found near the depth of test size of *G. menardii* (Fig. 8). Remarkably, neither the inflection points (for *G. calida* at 57 m and for *G. menardii* at 111 m) nor the bases of the productive zone (for *G. calida* at 72 m and for *G. menardii* at 132 m) appear to coincide with any particular hydrographic feature in the water column. It may be anticipated that temperature, light or food availability may limit the depth distribution of these species rather than the position of the thermocline or the fluorescence maximum.

Station 920 (at the same location as 310) reflects non-upwelling NE monsoon conditions of February 1993 (Figs 3 and 10). Contrasting the hydrography during upwelling, the DCM and thermocline were found at different depths in the water column. The surface mixed layer is *c.* 45 m thick and its base coincides with the DCM. Nitrate rapidly increases to 10–15 μM below the depleted surface mixed layer. At this station the main thermocline was found at 99 m. All species show a maximum of the shell concentration close to the sea surface. Although less pronounced, the concentration profiles consistently indicate a subsurface maximum too. Surface maxima are associated with small, immature specimens, whereas the deeper maxima, associated with the DCM, represent the larger (adult) specimens. The base of the productive zone is consistently found in the zone between the mixed layer (DCM) and

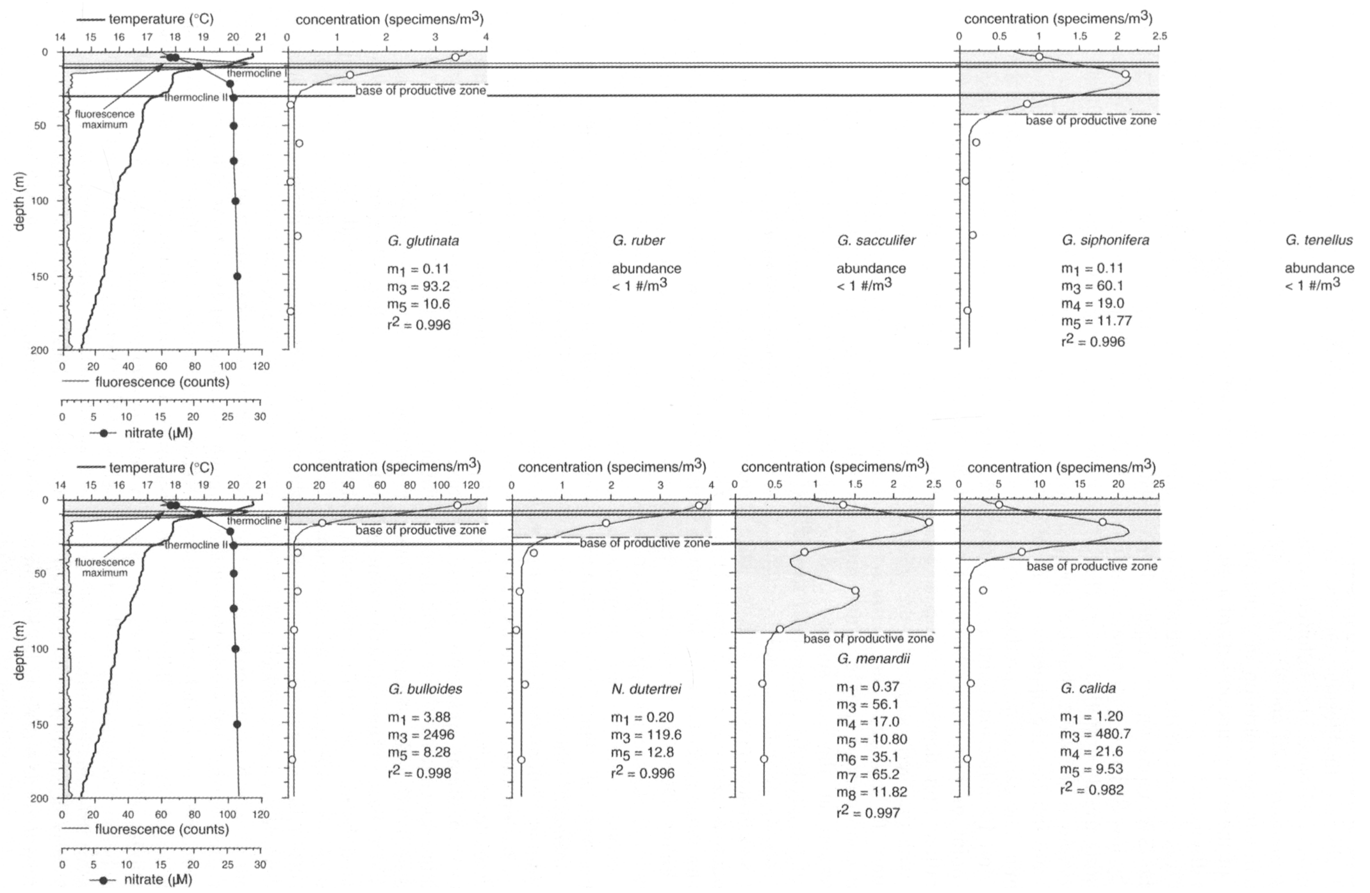

Fig. 7. CTD profile of station 310 in the centre of upwelling during the SW monsoon in August 1992, showing temperature, fluorescence, nitrate concentration and the shell concentration profiles of the most abundant species. The low temperatures and very high nitrate availability at the surface, indicating freshly upwelled waters, should be noted. m_1 represents the value of the settling flux concentration (C_{SF}), m_3 represents the total surface-area under the Gaussian distribution, m_4 represents the centre of the Gaussian distribution (c) and indicates the depth of the maximum in the shell concentration profile, whereas m_5 represents the width of the Gaussian distribution (σ). Note that m_6, m_7 and m_8 have similar meaning as m_3, m_4 and m_5 but now refer to the second Gaussian distribution that is used to fit a second (deepest) maximum in the shell concentration profile.

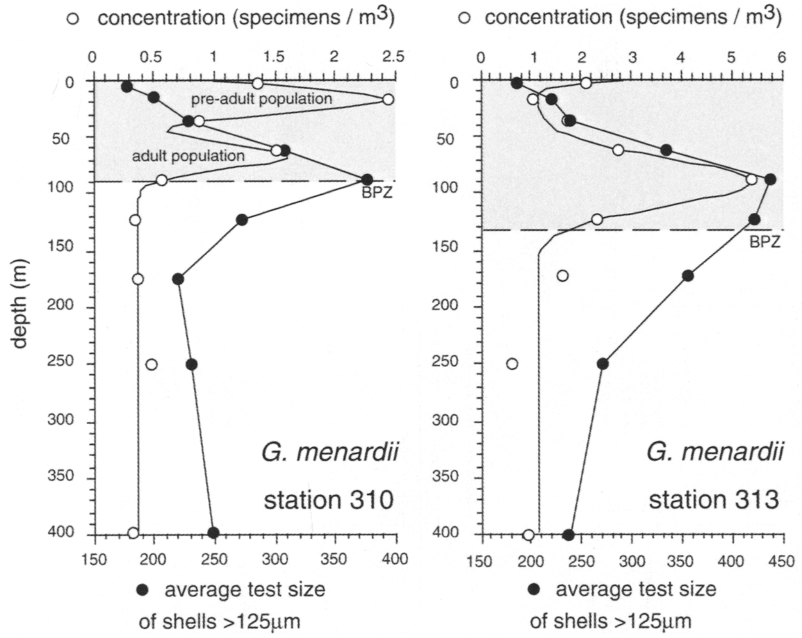

Fig. 8. Vertical shell concentration profiles and average test size of *G. menardii* at stations 310 and 313 (SW monsoon in August 1992). The average test size of *G. menardii* increases with depth down to the base of the productive zone, as defined by fitting the shell concentration profile, and indicates that specimens are growing down to the base of the productive zone. Below the productive zone the specimens are dead and have lost their ability to counter gravitational settling. Because larger (heavier) specimens settle faster to the sea floor the average test size decreases below the productive zone.

the thermocline, for both upwelling as well as non-upwelling species. However, concentrations of UA species (*G. bulloides*, *N. dutertrei*and *G. menardii*) are low compared with those of TA species (*G. glutinata*, *G. ruber*, *G. sacculifer*, *G. siphonifera* and *G. tenellus*). The shell concentration profile of *G. calida* is very different from that of the other species and our curve fitting procedure suggests that the base of the productive zone is at *c.* 280 m (i.e. far below the thermocline).

Station 917 (at the same location as 313), reflects non-upwelling conditions of February 1993 (Figs 3 and 11). At this station the mixed layer is about 15 m thick, whereas the DCM is present at 29 m and appeared to coincide with the first measurable increase in nitrate. The thermocline was found at 96 m. Most species show a subsurface maximum, between the DCM and the thermocline, with strikingly similar concentration profiles of *G. bulloides*, *G. glutinata*, *N. dutertrei* and *G. ruber*. *G. sacculifer*, however, shows a shell concentration maximum near the sea surface. It is known that *G. sacculifer* migrates vertically during ontogeny between the chlorophyll maximum and the sea surface (Bijma *et al.* 1990; Bijma *et al.* 1994; Hemleben & Bijma 1994) and we suggest that the *G. sacculifer* population at this station is relatively young. The base of the productive zone is consistently found between 59 and 74 m. Although no curve fit for the shell concentration profile of *G. calida* could be established by our model, the shell concentration profile suggests that for this species the base of the productive zone is below 200 m.

Depth habitat and $\delta^{18}O_{shell}$

The shell concentration profiles suggest that living specimens may be found in a zone ranging from the sea surface to the base of the productive zone. It can thus be expected that, within the productive zone, the oxygen isotope composition of the shells increases with depth because of continuing shell growth at lower temperatures. Below a certain depth level, however, the oxygen isotope composition should remain constant because shell growth has ceased. This, of course, is true only if upper ocean conditions are more or less constant for the period of the observations. It is interesting to know what depth level of the upper water column is represented by the oxygen isotope composition of the shells. To establish a relationship between

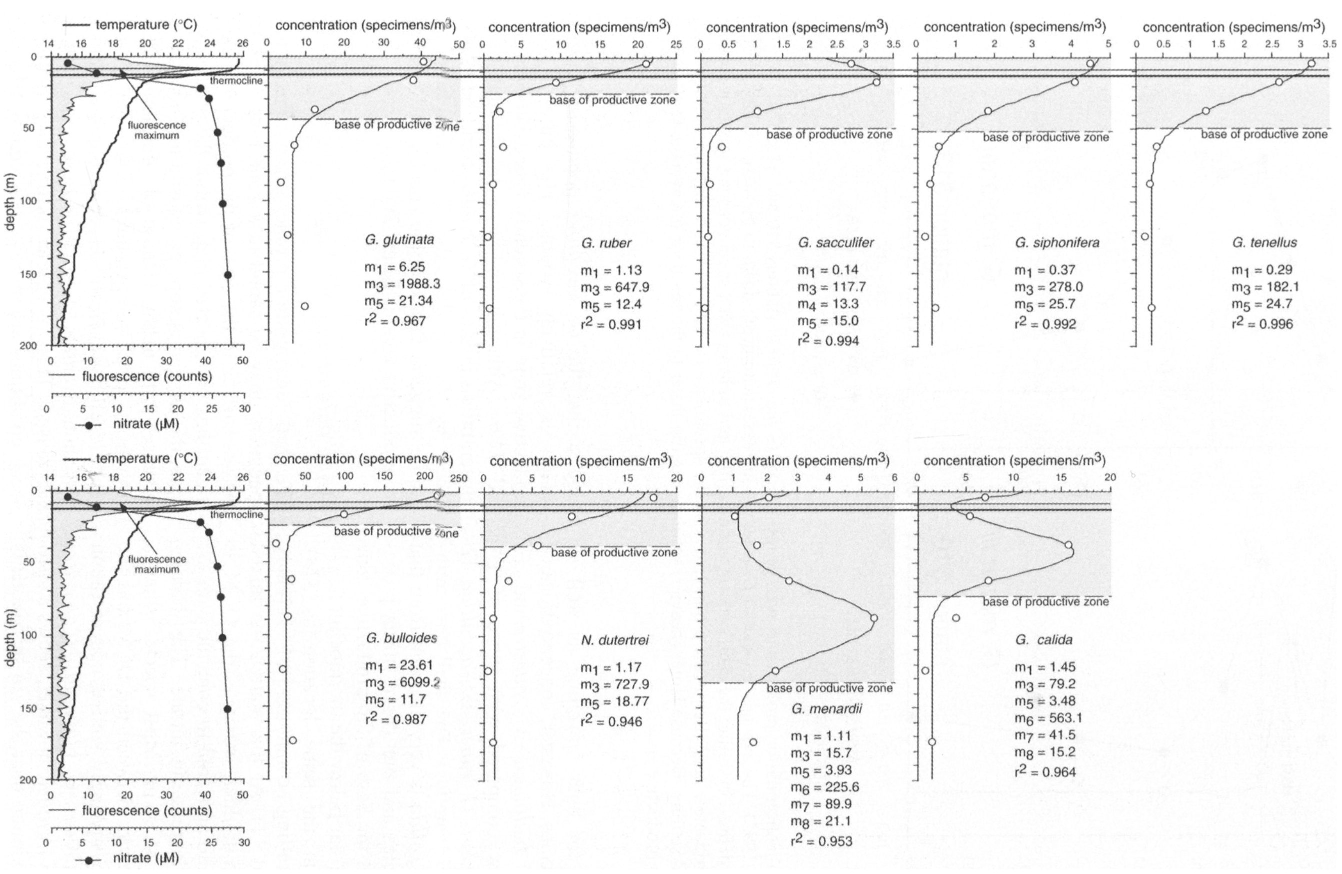

Fig. 9. CTD profile of station 313 in a warm core eddy during the SW monsoon in August 1992, showing temperature, fluorescence, nitrate concentration profile and the shell concentration profiles of the most abundant species at this station. The lower nitrate availability and higher temperature of the mixed layer, indicating more aged surface waters relative to station 310, should be noted. m_1 represents the value of the settling flux concentration (C_{SF}), m_3 represents the total surface-area under the Gaussian distribution, m_4 represents the centre of the Gaussian distribution (c) and indicates the depth of the maximum in the shell concentration profile, whereas m_5 represents the width of the Gaussian distribution (σ). Note that m_6, m_7 and m_8 have similar meaning as m_3, m_4 and m_5 but now refer to the second Gaussian distribution that is used to fit a second (deepest) maximum in the shell concentration profile.

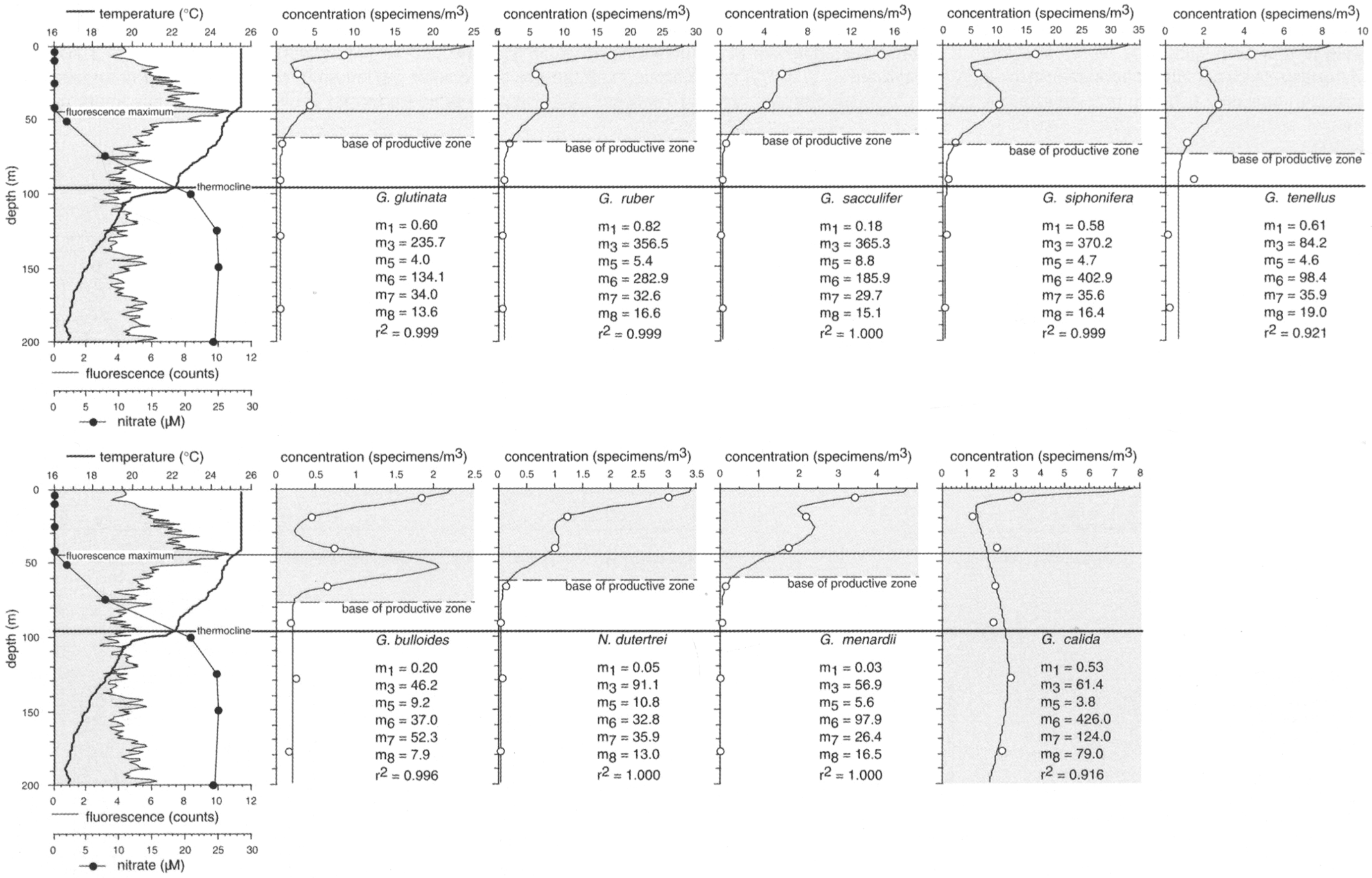

Fig. 10. CTD profile of station 920 during the NE monsoon in February 1993, showing temperature, fluorescence, nitrate concentration and the shell concentration profiles of the most abundant species at this station. In contrast to upwelling conditions the fluorescence maximum and thermocline are found at different depths in the water column. m_1 represents the value of the settling flux concentration (C_{SF}), m_3 represents the total surface-area under the Gaussian distribution, m_4 represents the centre of the Gaussian distribution (c) and indicates the depth of the maximum in the shell concentration profile, whereas m_5 represents the width of the Gaussian distribution (σ). Note that m_6, m_7 and m_8 have similar meaning as m_3, m_4 and m_5 but now refer to the second Gaussian distribution that is used to fit a second (deepest) maximum in the shell concentration profile.

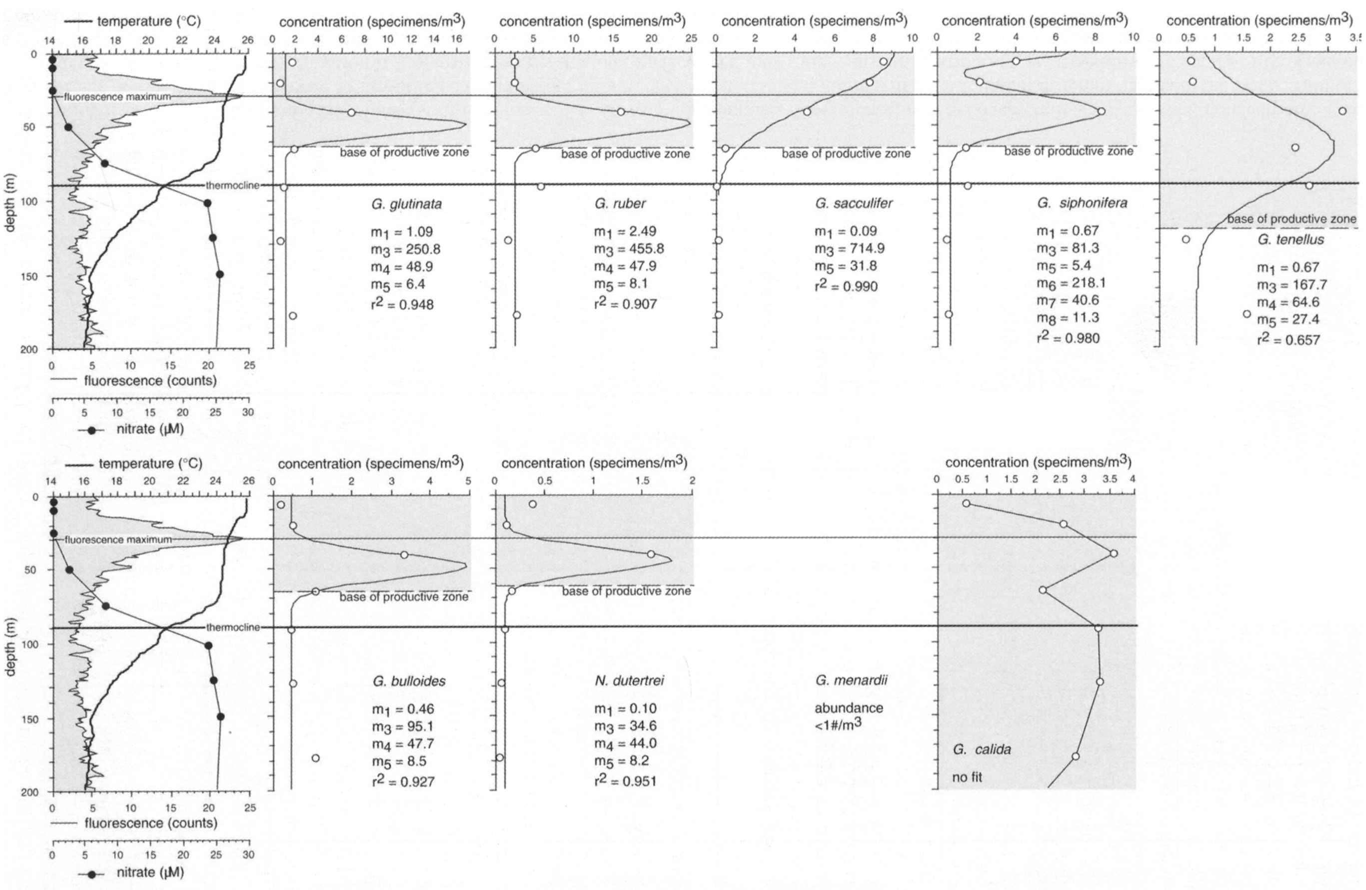

Fig. 11. CTD profile of station 917 during the NE monsoon in February 1993, showing temperature, fluorescence, nitrate concentration and the shell concentration profiles of the most abundant species at this station. m_1 represents the value of the settling flux concentration (C_{SF}), m_3 represents the total surface-area under the Gaussian distribution, m_4 represents the centre of the Gaussian distribution (c) and indicates the depth of the maximum in the shell concentration profile, whereas m_5 represents the width of the Gaussian distribution (σ). Note that m_6, m_7 and m_8 have similar meaning as m_3, m_4 and m_5 but now refer to the second Gaussian distribution that is used to fit a second (deepest) maximum in the shell concentration profile.

the shell concentration profile and calcification temperatures of specimens in the water column (T_c), the oxygen isotope composition of *G. bulloides* was measured at stations 310, 313, 917 and 920. All $\delta^{18}O_{shell}$ measurements are converted into calcification temperature following the methods discussed by Peeters *et al.* (2002). As we are interested in the calcification temperatures of the exported specimens, we excluded the measurements from the uppermost two plankton nets representing mostly living specimens. The obtained calcification temperatures (see Table 6) clearly indicate a shallower calcification depth during upwelling (stations 310 and 313) than during non-upwelling (stations 917 and 920), when the ocean is thermally stratified. The average calcification temperatures suggest that during upwelling *G. bulloides*calcifies in the upper 10–15 m and during non-upwelling between 50 and 60 m. These temperatures exactly correspond to the depth level in the shell concentration profile that is characterized by a rapid decline in the shell concentration (i.e. the inflection point). In addition, the total range in calcification temperatures corresponds to the expected *in situ* temperature range from the sea surface to the base of the productive zone.

Depth habitat and ambient temperatures

Above, we have shown that the average calcification temperature of *G. bulloides* corresponds to the temperature found at the inflection point in the concentration profile. It also has been shown that the total range of calcification temperatures corresponds to the temperature range from the sea surface to the base of the productive zone. However, it is known that the $\delta^{18}O$ of foraminifera from plankton tows have lower values than the $\delta^{18}O$ of the shells on the sea floor (Bé 1980; Curry & Matthews 1981; Duplessy *et al.* 1981). Secondary calcification (e.g. during gametogenesis at the end of the foraminiferal life cycle) and vital effects related to ontogenetic processes may explain this difference (e.g. Duplessy *et al.* 1981; Spero & Lea 1996; Bemis *et al.* 1998). Among others, we observe that the average test size of species is relatively small near the sea surface and increases with depth in the water column. This suggests that during their life cycle the specimens descent to deeper water while they grow larger. The $\delta^{18}O_{shell}$ thus represents an integrated signal over the productive zone.

If we assume that the relationship between the oxygen isotope composition and the shell concentration profile can be used for other species as well, we may use the depth of the inflection point to estimate the expected average $\delta^{18}O_{shell}$. In Figs 12 and 13 we plotted, for various species, the inflection point of the shell concentration profile on the temperature profile. We have limited the ambient temperature ranges for the species to those temperatures found in a range of 1 SD above and below the inflection point. This represents the range from the maximum in the shell concentration profile to the base of the productive zone.

Upwelling conditions. Figure 12 shows the expected average calcification temperature for various species of planktic foraminifera at upwelling stations 310 and 313. For each species the inflection point is plotted on the temperature profile (see also Fig. 4). The vertical bars indicate the inferred depth habitat from the concentration profile, ranging from the maximum in the concentration profile to the base of the productive zone. The horizontal bars indicate the range in ambient temperatures that will be recorded in the oxygen isotope composition of the shells. Most of the species inhabit the upper 35 m of the water column. Inflection points are consistently found below the fluorescence maximum. Species such as *G. bulloides*, *G. glutinata*, *N. dutertrei* and *G. ruber* show the shallowest depth habitats. At station 310 ambient temperatures range from 20.7 °C at the sea surface, to as low as 17.7 °C. At station 313, these species live at temperatures ranging from 25.8 °C to 18.5 °C. The inflection points of *G siphonifera*, *G. calida* and *G. sacculifer* are found deeper in the water column between 20 and 57 m, reflecting temperatures down to 16.8 °C. At both stations *G. menardii* shows the deepest habitat. Its oxygen isotope composition will reflect temperatures below the main thermocline, i.e. between 16.7 and 15.5 °C.

Non-upwelling conditions. Figure 13 illustrates the depth ranges and associated temperatures for various species of planktic foraminifera at non-upwelling stations 920 and 917. At station 920, the fluorescence maximum coincides with the base of the mixed layer. Although there is a temperature gradient starting directly below the surface mixed layer at 40 m, the main thermocline is present at *c.* 100 m. In contrast to the upwelling conditions, the inflection points of species are consistently found between 40 and 60 m, except for the inflection point of *G. sacculifer* at station 917, which is found slightly shallower. The species thus represent temperatures below the surface mixed layer and above the main thermocline. The total temperature range in the upper 70 m at station 920 is only 1.7 °C, from 25.4 °C at the surface to 23.7 °C at 70 m. At station 917 the fluorescence maximum and mixed layer are decoupled. The onset of a small thermocline, di-

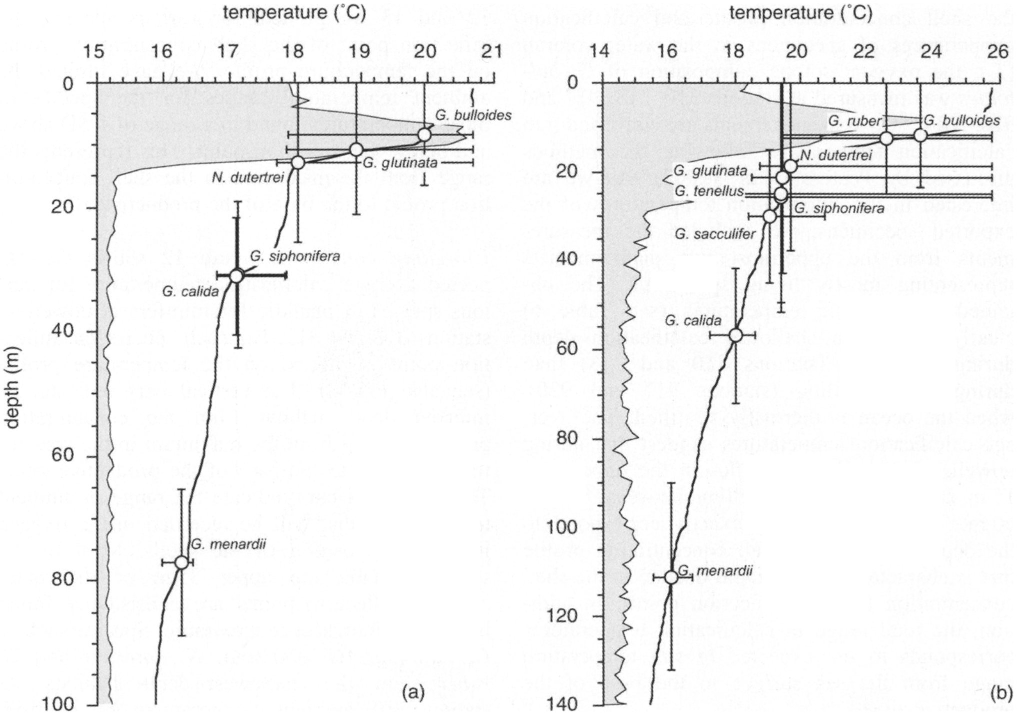

Fig. 12. Depth habitat and ambient temperatures for various species of planktic foraminifera at upwelling stations: (**a**) 310; (**b**) 313. For each species, the inflection point of the shell concentration profile is plotted on the temperature profile. This temperature will be reflected in the mean oxygen isotope composition of the species. Horizontal bars indicate the ambient temperature for each species. The vertical bars indicate the depth habitat of adult specimens as inferred from curve fitting, and range from the level at which the maximum concentration is found to the base of the productive zone. The shaded area shows the fluorescence profile.

rectly below the mixed layer, is found above the DCM. Because inflection points of species are present between 50 and 60 m, all species reflect the same ambient temperature of 24.2 °C. Only *G. sacculifer* shows a shallower inflection point at the depth of the DCM and will reflect slightly higher temperatures than the other species. The base of the productive zone of all species is consistently found at about 60–65 m.

Standing stock

The size of the standing stock (SS_{COR}) may be interpreted as a measure of the success of a given species in response to environmental conditions. It can be expected that a high standing stock will produce a high shell flux (i.e. C_{SF}), whereas a low standing stock will produce a low shell flux. If shell production did not change with time, the standing stock would produce a constant 'rain' of shells to the sea floor (steady-state conditions). Consequently, one would expect to find a species-specific relationship between the integrated standing stock and the concentration of shells below the productive zone (i.e. C_{SF}). To test this hypothesis, we have plotted the standing stocks of various species (SS_{COR}) v. C_{SF} (Fig. 14b). Because both the size of the standing stock and C_{SF} vary over several orders of magnitude, we used logarithmic scales to visualize the data. For this figure, we used the data tabulated in Table 5. We found a positive relationship between SS_{COR} and C_{SF} for all species. Apparently, higher standing stocks indeed correspond to a higher export flux. However, the relationship between standing stock and export flux may differ with species. At a given size of the standing stock, species such as *G. bulloides*, *G. glutinata*, *G. ruber* and possibly *N. dutertrei* show a higher settling flux concentration compared with *G. menardii*, *G. sacculifer*, *G. calida* and *G. siphonifera*. This suggests that turnover rates are higher or settling speeds of these species are lower. Although the relationship between the standing stock and the settling flux might be affected by different processes, it will provide the answer to the turnover rates of differ-

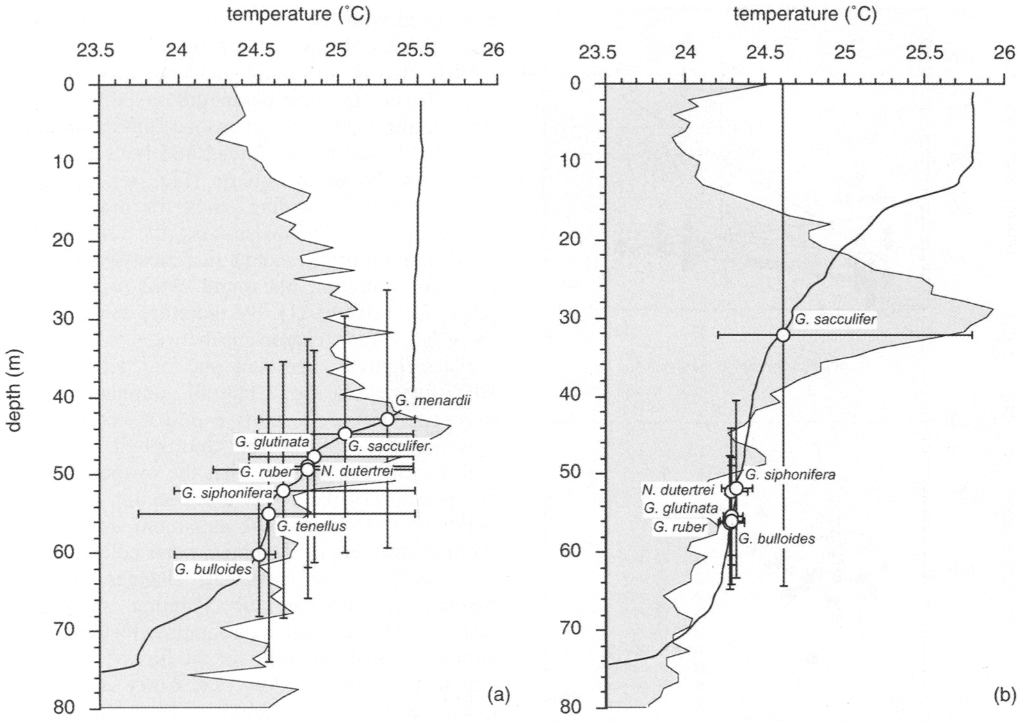

Fig. 13. Depth habitat and ambient temperatures for various species of planktic foraminifera at non-upwelling stations: (**a**) 920; (**b**) 917. For each species, the inflection point of the distribution profile is plotted on the temperature profile. The vertical bars indicate the depth habitat of adult specimens as inferred by Gaussian fitting, from the level at which the maximum concentration is found to the base of the productive zone. Horizontal bars indicate the ambient temperature for each species. The shaded area shows the fluorescence profile.

ent species. For such an approach, however, one would need plankton tow data and sediment trap observations from one location.

Discussion

Planktic foraminifera respond to changing environmental conditions of the upper water column. From a palaeoceanographic point of view it is important to know how biological and physical features of the upper water column (e.g. depth of chlorophyll maximum, mixed layer depth, thermocline depth) control the abundance and the calcification depths of various species. Bé & Hutson (1977) noted that: ‘The net effect of depth stratification of species has important implications for paleoecological analysis in that species living at different depths (with different environmental conditions) are mixed together in the same dead assemblage on the sea floor’.

Plankton tow studies in the tropical Atlantic and Pacific Ocean indicate that mixed layer depth, thermocline depth, integrated primary productivity and light attenuation levels may control the absolute abundance and depth habitat of planktic foraminifera (Ravelo & Fairbanks 1992; Watkins *et al.* 1998). The definition of the base of the productive zone, introduced in this paper, provides an independent tool to estimate the depth of calcification for various species. Estimates of the standing stock and base of the productive zone may help to identify the environmental conditions that control the abundance and vertical distribution of a given species.

Our plankton tow data show that planktic foraminifera, collected during the two monsoon seasons, do not have an absolute depth habitat but rather live at depths directly related to the local hydrography. This observation is in agreement with previous work in other areas (e.g. Ravelo & Fairbanks 1992; Thunell & Reynolds-Sautter 1992). In general, most (non-globorotaloid) species appear to have a shallower habitat during upwelling (SW monsoon season) than during non-upwelling (NE monsoon season). The environmental parameters controlling the depth habitat, however, may vary depending on the species. Symbiont-bearing species such as *G. sacculifer*

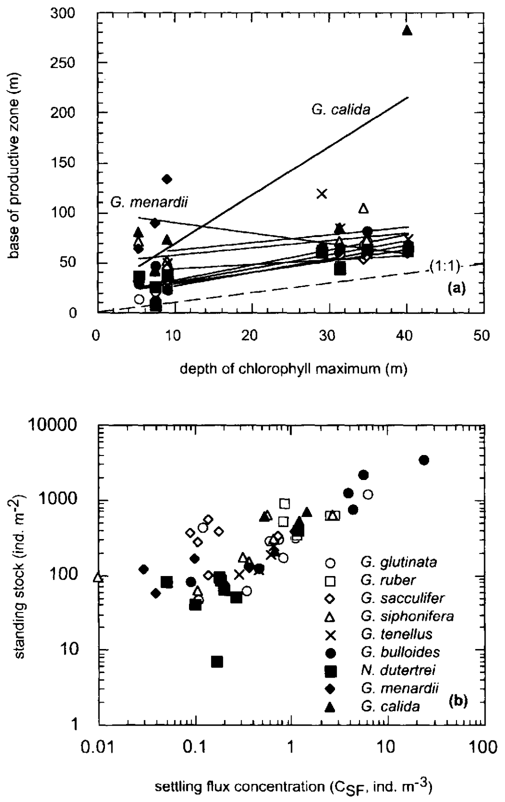

Fig. 14. (**a**) Scatter plot showing that the depth of the chlorophyll maximum and the base of the productive zone are positively correlated for most species. The species *G. menardii*, however, shows a negative relationship. (**b**) Relationship between the standing stock (SS_{COR}) and the shell concentration below the productive zone (C_{SF}). Higher standing stocks correspond to higher shell concentrations below the productive zone.

and *G. ruber* may obtain nutrition from their symbionts and proliferate in oligotrophic environments such as found in the mixed layer. For these species, light availability or mixed layer temperature may control their distribution (Mulitza *et al.* 1998). On the other hand, the availability of particulate food may be more important for other species such as, for example, *G. bulloides* (Watkins *et al.* 1996). To define whether a certain hydrographic state of the upper ocean is favourable for a given species, one should consider the size of the standing stock. Fairbanks & Wiebe (1980) showed that the DCM plays an important role in the vertical distribution patterns of planktic foraminifera in the upper water column. It provides the primary food source for most foraminiferal species, and highest concentrations are often associated with the DCM. Off the Arabian Peninsula, the DCM appears to be close to the sea surface during upwelling and coincides with the main thermocline just below the mixed layer (Fig. 2e). During winter (NE monsoon) the thermocline and DCM may be decoupled and both are found deeper in the water column (Fig. 3e). Although the size of the standing stock for most species differs between the two seasons, the vertical shell concentration profiles show that most species have their concentration maximum close to the DCM (Figs. 7, 9, 10 and 11). We therefore conclude that there is a direct relationship between the depth of the chlorophyll maximum and the depth of the BPZ. Figure 14a shows that all dominant species, except *G. menardii*, show a positive relationship between the depth of the chlorophyll maximum and the BPZ, suggesting that the oxygen isotopic composition of the shells is a function of (1) the depth of the chlorophyll maximum and (2) the thermal structure of the upper water column.

As well as the (seasonal) changes in depth habitat, the size of the standing stock also responds to the local hydrography, resulting in a strong seasonal variability of the flux of foraminiferal shells to the sea floor (e.g. Curry *et al.* 1992; Conan & Brummer, 2000). The most striking seasonal change in the size of the standing stock is observed in *G. bulloides*. Previous studies have shown that this species is the best indicator for upwelling (Anderson & Prell 1991; Brock *et al.* 1992; Curry *et al.* 1992; Anderson & Prell 1993; Naidu & Malmgren 1996*a*, *b*). During upwelling conditions, the standing stock varied between 760 and 3500 ind. m^{-2}, whereas during the non-upwelling period, the standing stock did not exceed 140 ind. m^{-2}. Remarkably, the size of the standing stock of *G. bulloides* and the depth of the DCM are negatively correlated (Fig. 15). During upwelling conditions this species inhabits the uppermost part of the water column and its inflection point coincides with the DCM, suggesting that food availability is the most important environmental parameter controlling the size of the standing stock. Although the reproductive cycle and thus the standing stock of *G. bulloides*may be related to lunar periodicity in regions with relatively stable upper ocean conditions (Schiebel *et al.* 1997), in the Arabian Sea the size of its standing stock is mainly controlled by the process of upwelling and related phyto- and zooplankton blooms, which serve as food for this species. Other abundant species in the Arabian Sea, such as *G. siphonifera*, *G. ruber* and *G. sacculifer*, show a positive correlation with the depth of the DCM. These are all symbiont-bearing species, which are most abundant in the surface mixed layer (Watkins *et al.* 1996).

As a result of the seasonal changes in hydrography, the faunal assemblages found during the two monsoon seasons clearly differ from one another. During the SW monsoon, species from the upwelling assemblage, which are also characteristic for cold-water regions at high latitudes (Bé & Tolderlund 1971) dominate in the faunal assemblage, whereas during the NE monsoon the faunal assemblage is dominated by species from the tropical assemblage. It is known, however, that during the SW monsoon, fluxes of most species increase (Curry *et al.* 1992; Conan & Brummer, 2000). Our data indicate that, during upwelling, species from the tropical assemblage are not present in the centre of upwelling, but are found in 'aged' upwelled waters, with lower nitrate concentrations and higher sea surface temperatures (i.e. station 313, Figs 2a and 5). The tropical assemblages may thus be found predominantly in warm-water eddies. These eddies mostly have a shallow chlorophyll maximum and therefore during upwelling species from the tropical assemblage also reflect shallower water column properties than during non-upwelling.

A small sample from the sedimentary record often represents a time span from tens to hundreds of years. Here, the shells of foraminifera that were produced during various seasons are mixed together in one fossil assemblage. This study shows that a seasonal decomposition of the fossil assemblage is feasible. The abundance and stable isotopic composition of species that were produced during different times of the year may be used to reconstruct the palaeoceanographic conditions of the two monsoon seasons. Potentially, such an approach would allow for a reconstruction of sea surface temperature, biological productivity and water column stratification of both monsoon seasons. However, for such an approach, it is essential to know the turnover rates of each of the species. Only when shell fluxes of the various species are coupled to standing stock estimates will it be possible to improve palaeoceanographic interpretations of monsoon history. We suggest that future work should concentrate on the relationship between living planktic foraminifera and their export flux, to quantify turnover rates for the various species.

Conclusions

In this study, we compared the depth habitat and seasonal distribution of living foraminifera in the upwelling area off the Arabian Peninsula in response to monsoon-controlled hydrographic changes. The following conclusions are drawn from this study.

(1) In the area off Oman–Yemen, the faunal assemblage, shell concentrations, standing stock and depth habitat of planktic foraminifera change seasonally. Because hydrographic changes in this area are directly coupled to the monsoon system, the changes in the faunal assemblage and isotopic composition of individual species allow reconstruction of surface water conditions and monsoon history over longer time scales.

(2) Factor analysis on 15 species yields three faunal assemblages: an upwelling assemblage, a tropical assemblage and a subsurface assemblage. A fourth factor represents the distribution pattern of *Globigerina falconensis*. This species is mainly found during NE monsoon conditions and inhabits subsurface waters. Consequently, this species is the best faunal indicator of NE monsoon conditions.

(3) Living planktic foraminifera do not have an absolute depth habitat (calcification depth), but rather live at depths related to the local hydrography. Most shallow-dwelling species have a shallower habitat during upwelling (SW monsoon) than during non-upwelling (NE monsoon). The depth of the chlorophyll maximum appears to be an important environmental parameter controlling the depth habitat of species.

(4) The shell concentration profile of most planktic foraminifera may be described by a Gaussian distribution model that can be used to calculate the base of the productive zone, reflecting the boundary between the productive and settling flux zone. For non-globorotaloid species, the base of the productive zone depends on the depth of the DCM. Below the productive zone the shell concentration is low and represents dead specimens settling to the sea floor.

(5) The standing stock varies seasonally and is related to the shell concentration below the productive zone, representing the shells of dead specimens settling to the sea floor. Higher standing stocks correspond to higher settling flux concentrations, suggesting a direct relationship between shell production and export flux.

(6) During upwelling, tropical species do not proliferate in the centre of upwelling. However, high abundances of these species may be found in relatively warm-water eddies or upwelling filaments.

(7) The standing stock of *G. bulloides*correlates negatively with mixed layer depth and the depth of the chlorophyll maximum. This suggests that food availability may be the most important environmental parameter controlling the size of the standing stock. The standing stocks of species that possess photosynthetic symbionts, such as *G. sacculifer*, *G. siphonifera* and *G. ruber,* correlate

Table 5. *Results of calculations*

	Upwelling stations							Non-upwelling stations					
Station 313 (D)	SS	SS_{COR}	C_{SF}	z_{MAX}	z_i	z_{BPZ}	Station 917 (D)	SS	SS_{COR}	C_{SF}	z_{MAX}	z_i	z_{BPZ}
G. glutinata	1215	1082	6.25	0	21	43	*G. glutinata*	312	279	1.09	49	55	62
G. ruber	337	323	1.13	0	12	25	*G. ruber*	615	535	2.49	48	56	64
G. sacculifer	99	96	0.14	13	28	43	*G. sacculifer*	363	360	0.09	0	32	64
G. siphonifera	152	142	0.37	0	26	51	*G. siphonifera*	296	275	0.67	41	52	63
G. tenellus	101	94	0.29	0	25	49	*G. tenellus*	244	204	0.67	65	92	119
G. bulloides	3463	3187	23.61	0	12	23	*G. bulloides*	123	108	0.46	48	56	65
N. dutertrei	391	369	1.17	0	19	38	*N. dutertrei*	40	37	0.10	44	52	60
G. menardii	375	302	1.11	90	111	132	*G. menardii*						
G. calida	691	638	1.45	42	57	72	*G. calida*						
Station 310 (D)							Station 920 (D)						
G. glutinata	47	46	0.11	0	11	21	*G. glutinata*	286	267	0.60	0	48	61
G. ruber							*G. ruber*	509	482	0.82	0	49	66
G. sacculifer							*G. sacculifer*	370	365	0.18	0	45	60
G. siphonifera	60	58	0.11	19	31	43	*G. siphonifera*	612	592	0.58	0	52	68
G. tenellus							*G. tenellus*	183	161	0.61	0	55	74
G. bulloides	1255	1223	3.88	0	8	17	*G. bulloides*	73	66	0.20	0	60	68
N. dutertrei	65	62	0.20	0	13	26	*N. dutertrei*	81	79	0.05	0	49	62
G. menardii	123	107	0.37	17	77	89	*G. menardii*	120	119	0.03	0	43	59
G. calida	513	489	1.20	22	31	41	*G. calida*	596	522	0.53	0	203	282
Station 311 (S)							Station 918 (S)						
G. glutinata							*G. glutinata*[1]	172	*144*	*0.82*	33	51	68
G. ruber							*G. ruber*[2]						
G. sacculifer							*G. sacculifer*	266	263	0.11	0	26	52
G. siphonifera							*G. siphonifera*[1]	529	n.d	.n.d	.37	70	104
G. tenellus							*G. tenellus*[2]						
G. bulloides	758	733	4.31	0	6	12	*G. bulloides*						
N. dutertrei	7	6	0.17	0	4	7	*N. dutertrei*						
G. menardii							*G. menardii*						
G. calida							*G. calida*						

Station 308 (S)							Station 919 (S)						
G. glutinata	63	60	0.35	0	7	14	*G. glutinata*[1]	292	*266*	*0.74*	43	57	71
G. ruber							*G. ruber*[1]	615	*530*	*2.76*	42	52	61
G. sacculifer							*G. sacculifer*[1]	320	*299*	*0.74*	39	47	55
G. siphonifera[1]	95	*95*	*0.01*	28	49	70	*G. siphonifera*[1]	620	*521*	*2.72*	46	60	73
G. tenellus							*G. tenellus*[1]	119	*105*	*0.46*	38	49	60
G. bulloides	2173	2094	5.52	0	14	29	*G. bulloides*[1]	140	n.d	.n.d	46	63	81
N. dutertrei	84	81	0.19	0	18	36	*N. dutertrei*[1]	52	*44*	*0.27*	40	52	63
G. menardii[1]	165	*162*	*0.10*	0	32	63	*G. menardii*						
G. calida[1]	667	*667*	*0.00*	0	40	79	*G. calida*						
							Station 922 (S)						
							G. glutinata	438	434	0.12	0	30	59
							G. ruber	899	879	0.85	0	23	46
							G. sacculifer	550	547	0.14	0	23	46
							G. siphonifera[1]	172	*160*	*0.32*	35	53	71
							G. tenellus[1]	205	n.d	n.d	47	66	85
							G. bulloides[1]	81	*78*	*0.09*	0	32	65
							N. dutertrei	93	89	0.18	0	22	43
							G. menardii	57	55	0.04	30	45	61
							G. calida[1]	203	*174*	*0.69*	42	63	84

[1] C_{SF} and C_{COR} not well defined.

[2] Shell concentration profile does not allow a curve fit.

Calculations were carried out on: standing stock (*SS*) following equation (9), corrected standing stock (SS_{COR}) following equation (10), settling shell concentration (C_{SF}) following equation (6), depth of maximum shell concentration (z_{MAX}) following equation (6), depth of shell concentration inflection point (z_I) following equation (8) and depth of the productive zone (z_{BPZ}) following equation (7). D, station with deep cast (0–500 m); S, station with shallow cast (0–100 m). Stations with a deep multi-net in general yield better estimates for C_{SF}, *SS* and SS_{COR}.

Table 6. *Calcification temperature statistics of* G. bulloides *and corresponding depth levels*

Station	T_c average (°C)	SD (°C)	T_c min. (°C)	T_c max. (°C)	*n*	Average calcif. depth (m)	Maximum depth (m)	Shell concentration inflection point (m)
310	19.8	0.6	18.6	21.1	12	10	12	8
313	23.6	0.3	23.0	24.3	15	12	13	12
917	24.3	1.0	23.3	25.5	4	53	76	56
920	24.5	0.1	24.3	24.6	3	61	64	60

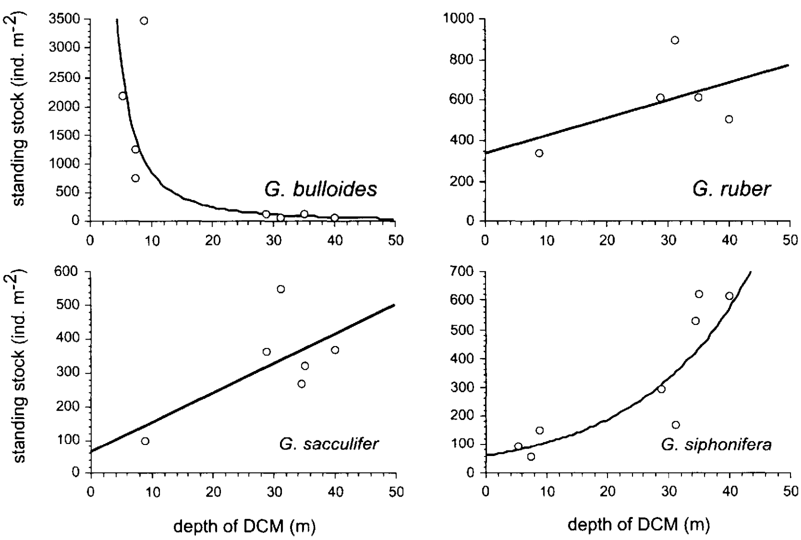

Fig. 15. The integrated standing stock of living *Globigerina bulloides* correlates inversely with the depth of the chlorophyll maximum. The standing stock of symbiont-bearing species such as *Globigerinella siphonifera* and *Globigerinoides sacculifer* correlates positively with the depth of the chlorophyll maximum.

positively with mixed layer depth and the depth of the chlorophyll maximum.

The Netherlands Indian Ocean Programme was funded and coordinated by the Netherlands Marine Research Foundation (SOZ) of the Netherlands Organization for Scientific Research (NWO). We thank Captain J. de Jong, technicians and crews of R.V. *Tyro*. J. Kranenborg and W. van Raaphorst are thanked for helpful suggestions and discussion. We are grateful to J. van Hinte for his critical comments on an earlier version of this work. We much appreciate the constructive reviews of K. Darling and L. Sautter. This is Publication 3649 of the Netherlands Institute for Sea Research (NIOZ).

References

Anderson, D.M. & Prell, W.L. 1991. Coastal upwelling gradient during the Late Pleistocene. *In:* Prell, W.L. & Nitsuma, N. (eds) *Proceedings of the Ocean Drilling Program, Scientific Results, 117.* Ocean Drilling Program, College Station, TX, 265–275.

Anderson, D.M. & Prell, W.L. 1993. A 300 kyr record of upwelling off Oman during the Late Quaternary: evidence of the Asian southwest monsoon. *Paleoceanography*, **8**, 193–208.

Anderson, D.M. & Thunell, R.C. 1993. The oxygen-isotope composition of tropical ocean surface water during the last deglaciation. *Quaternary Science Reviews*, **12**, 465–473.

Anderson, D.M., Brock, J.C. & Prell, W.L. 1992. Physical upwelling processes, upper ocean environment and the sediment record of the southwest monsoon. *In:* Summerhays, C.P., Prell, W.L. & Emeis, K.c. (eds) *Upwelling Systems: Evolution since the Early Miocene.* Geological Society, London, Special Publications, **64**, 121–129.

Banse, K. 1994. On the coupling of hydrography, phytoplankton, zooplankton, and settling organic particles offshore in the Arabian Sea. *In:* Lal, D. (eds) *Biogeochemistry of the Arabian Sea.* Indian Academy of Sciences, Bangalore, 27–63.

Bé, A.W.H. 1967. Foraminifera families: Globigerinidae and Globorotaliidae. *In:* Fraser, J. H. (ed.) *Fiches d'Identification du Zooplankton, sheet 108.* Conseil Permanent International pour l'Exploration de la Mer, Charlottenlund, Denmark, 1–3.

Bé, A.W.H. 1980. Gametogenetic calcification in a spinose planktonic foraminifer. Globigerinoides sacculifer (Brady) *Marine Micropaleontology,* **5**, 283–310.

Bé, A.W.H. & Hutson, W.H. 1977. Ecology of planktonic foraminifera and biogeographic patterns of life and fossil assemblages in the Indian Ocean. *Micropaleontology,* **23**, 369–414.

Bé, A.W.H. & Tolderlund, D.S. 1971. Distribution and ecology of living planktonic foraminifera in surface waters of the Atlantic and Indian Oceans. *In:* Funnell, B.M. & Riedel, W.R. (eds) *Micropaleontology of Oceans.* Cambridge University Press, Cambridge, 105–149.

Bemis, B.E., Spero, H.J., Bijma, J. & Lea, D. 1998. Reevaluation of the oxygen isotopic composition of planktonic foraminifera: experimental results and revised paleotemperature equations. *Paleoceanography,* **13**, 150–160.

Berger, W.H. 1969. Ecologic patterns of living planktonic foraminifera. *Deep-Sea Research,* **169**, 1–24.

Berger, W.H. 1971. Planktonic foraminifera: sediment production in an oceanic front. *Journal of Foraminiferal Research,* **1**, 95–118.

Bijma, J. & Hemleben, C. 1994. Population dynamics of the planktic foraminifer *Globigerinoides sacculifer* (Brady) from the central Red Sea. *Deep-Sea Research I,* **41**, 485–510.

Bijma, J., Erez, J. & Hemleben, C. 1990. Lunar and semi-lunar reproductive cycles in some spinose planktonic foraminifers. *Journal of Foraminiferal Research,* **20**, 117–127.

Bijma, J., Hemleben, C. & Wellnitz, K. 1994. Lunar-influenced carbonate flux of the planktic foraminifer *Globigerinoides sacculifer* (Brady) from the central Red Sea. *Deep-Sea Research, I,* **41**, 511–530.

Brock, J.C., McClain, C.R., Anderson, D.M., Prell, W.L. & Hay, W.W. 1992. Southwest monsoon circulation and environments of recent planktonic foraminifera in the northwestern Arabian sea. *Paleoceanography,* **7**, 799–813.

Brummer, G.-J.A. 1995. Plankton pump and multinet. *In:* Van Hinte, J.E., Van Weering, T.J.C. & Troelstra, S.R. (eds) *Tracing a Seasonal Upwelling: Report on Two Cruises of RV* Tyro *to the NW Indian Ocean in 1992 and 1993.* National Museum of Natural History, Leiden, **4**, 31–40.

Brummer, G.-J.A. & Kroon, D., 1988. *Planktonic foraminifers as tracers of ocean–climate history.* Ph.D. thesis, Free University Press Amsterdam.

Conan, S.M.-H. & Brummer, G.-J.A. 2000. Fluxes of planktic foraminifera in response to monsoonal upwelling on the Somalia Basin margin. *Deep-Sea Research II,* **47**, 2207–2227.

Coplen, T.B., Kendall, C. & Hopple, J. 1983. Comparison of stable isotope reference sample. *Nature,* **302**, 236–238.

Curry, W.B. & Matthews, R.K. 1981. Equilibrium ^{18}O fractionation in small size fraction planktic foraminifera: evidence from Recent Indian Ocean sediments. *Marine Micropaleontology,* **6**, 327–337.

Curry, W.B., Ostermann, D.R., Guptha, M.V.S. & Ittekot, V. 1992. Foraminiferal production and monsoonal upwelling in the Arabian Sea: evidence from sediment traps. *In:* Summerhays, C.P., Prell, W.L., & Emeis, K.C. (eds) *Upwelling Systems: Evolution since the Early Miocene.* Geological Society, London, Special Publications, **64**, 93–106.

Darling, K.F., Wade, C.M., Stewart, I.A., Kroon, D., Dingle, R. & Leigh-Brown, A.J. 2000. Molecular evidence for genetic mixing of Arctic and Antarctic subpolar populations of planktonic foraminifers. *Nature,* **405**, 43–47.

Deuser, W.G., Ross, E.H., Hemleben, C. & Spindler, M. 1981. Seasonal changes in species composition, numbers, mass, size, and isotopic composition of planktonic foraminifera settling into the deep Sargasso Sea. *Palaeogeography, Palaeoclimatology, Palaeoecology,* **33**, 103–127.

Duplessy, J.-C., Blanc, P.-L. & Bé, A.W.H. 1981. Oxygen-18 enrichment of planktonic foraminifera due to gametogenetic calcification below the euphotic zone. *Science,* **213**, 1247–1250.

Fairbanks, R.G. & Wiebe, P.H. 1980. Foraminifera and chlorophyll maximum: vertical distribution, seasonal succession, and paleoceanographic significance. *Science,* **209**, 1524–1526.

Furbish, D.J. & Arnold, A.J. 1997. Hydrodynamic strategies in the morphological evolution of spinose planktonic foraminifera. *Geological Society of America Bulletin,* **109**, 1055–1072.

Giraudeau, J. & Rogers, J. 1994. Phytoplankton biomass and sea-surface temperature estimates from sea-bed distribution of nannofossils and planktic foraminifera in the Benguela upwelling system. *Micropaleontology,* **40**, 275–285.

Hemleben, C. & Bijma, J. 1994. Foraminiferal population dynamics and stable carbon isotopes. *In:* Zahn, R., Pedersen, T.F., Kaminski, M.A. & Labeyrie, L. (eds) *Carbon Cycling in the Glacial Ocean: Constraints on the Ocean's Role in the Global Change.* NATO ASI Series I, **17**, 145–166.

Hemleben, C., Spindler, M. & Anderson, O.R. 1989. *Modern Planktonic Foraminifera.* Springer, Berlin.

Hut, G. 1987. *Stable Isotope Reference Samples for Geochemical and Hydrological Investigations. Consultants Group Meeting, 16-18.09.1985.* International Atomic Energy Agency, Vienna.

Hutson, W.H. & Prell, W.L. 1980. A paleoecological transfer function, FI-2, for Indian Ocean planktonic foraminifera. *Journal of Paleontology,* **54**, 381–399.

Ivanova, E.M., 2000. *Late Quaternary monsoon history and paleoproductivity of the western Arabian Sea.* PhD thesis, Free University Amsterdam.

Ivanova, E.M., Conan, S.M-H., Peeters, F.J.C. & Troelstra, S.R. 1999. Living *Neogloboquadrina pachyderma* sin and its distribution in the sediments from Oman and Somalia upwelling areas. *Marine Micropaleontology,* **36**, 91–107.

Kahn, M.I. & Williams, D.F. 1981. Oxygen and carbon isotopic composition of living planktonic foraminifera from the Northern Pacific Ocean. *Palaeogeography, Palaeoclimatology, Palaeoecology,* **33**, 47–69.

KEMLE-VON MÜCKE, S. 1994. *Oberflächenwasserstruktur und -zirkulation des Südostatlantiks im Spätquartär.* Berichte, Fachbereich Geowissenschaften, Universität Bremen, **55**.

KEMLE-VON MÜCKE, S. & OBERHÄNSLI, H. 1999. The distribution of living planktic foraminifera in relation to southeast Atlantic oceanography. *In:* FISCHER, G & WEFER, G. (eds) *Use of Proxies in Paleoceanography: Examples from the South Atlantic.* Springer, Berlin, 91–115.

KROON, D. & GANSSEN, G. 1989. Northern Indian Ocean upwelling cells and the stable isotope composition of living planktonic foraminifers. *Deep-Sea Research*, **36**, 1219–1236.

KROON, D., BEETS, K., MOWBRAY, S., SHIMMIELD, G. & STEENS, T. 1990. Changes in northern Indian Ocean monsoonal wind activity during the last 500 ka. *Memorie della Societa Geologica Italiana*, **44**, 189–207.

MCCREARY, J.P., KOHLER, K.E., HOOD, R.R. & OLSON, D.B. 1996. A four-component ecosystem model of biological activity in the Arabian Sea. *Progres in Oceanography,* **37**, 193–240.

MULITZA, S., WOLFF, T., PÄTZOLD, J., HALE, H. & WEFER, G. 1998. Temperature sensitivity of planktic foraminifera and its influence on the oxygen isotope record. *Marine Micropaleontology,* **33**, 223–240.

NAIDU, P.D. & MALMGREN, B.A. 1996*a*. Relationship between Late Quaternary upwelling history and coiling properties of *N. pachyderma* and *G. bulloides* in the Arabian Sea. *Journal of Foraminiferal Research*, **26**, 64–70.

NAIDU, P.D. & MALMGREN, B.A. 1996*b*. A high-resolution record of late Quaternary upwelling along the Oman Margin, Arabian Sea based on planktonic foraminifera. *Paleoceanography,* **11**, 129–140.

ORTIZ, J.D., MIX, A.C. & COLLIER, R.W. 1995. Environmental control of living symbiotic and asymbiotic foraminifera of the California Current. *Paleoceanography,* **10**, 987–1009.

OTTENS, J.J., 1992. *Planktic Foraminifera as indicators of ocean environments in the Northeast Atlantic.* PhD thesis, Free University Amsterdam.

PEETERS, F.J.C., BRUMMER, G.-J.A. & GANSSEN, G.M. 2002. The effect of upwelling on the distribution and stable isotope composition of *Globigerina bulloides* and *Globigerinoides ruber* (planktic foraminifera) in modern surface waters of the NW Arabian Sea. *Global and Planetary Change*, **35**, in press.

PEETERS, F.J.C., IVANOVA, E.M., CONAN, S.M.-H., BRUMMER, G.-J.A., GANSSEN, G.M., TROELSTRA, S.R. & VAN HINTE, J.E. 1999. A size analysis of planktic foraminifera from the Arabian Sea. *Marine Micropaleontology,* **36**, 31–63.

PRELL, W.L. & CURRY, W.B. 1981. Faunal and isotopic indices of monsoonal upwelling, Western Arabian Sea. *Oceanologica Acta*, **4**, 91–98.

PRELL, W.L., MURRAY, D.W., CLEMENS, S.C. & ANDERSON, D.M. 1992. Evolution and variability of the Indian Ocean summer monsoon: evidence from the Western Arabian Sea Drilling Programme. *In:* DUNCAN, R.A. ET AL. (eds) *Syntheses of Results from Scientific Drilling in the Indian Ocean.* Geophysical Monograph, American Geophysical Union, **70**, 447–469.

RAVELO, A.C. & FAIRBANKS, R.G. 1992. Oxygen isotopic composition of multiple species of planktonic foraminifera: recorders of the modern photic zone temperature gradient. *Paleoceanography,* **7**, 815–831.

RAVELO, A.C., FAIRBANKS, R.G. & PHILANDER, S.G.H. 1990. Reconstructing tropical Atlantic hydrography using planktonic foraminifera and an ocean model. *Paleoceanography,* **5**, 409–431.

ROSTEK, F., BARD, E., BEAUFORT, L., SONZOGNI, C. & GANSSEN, G. 1997. Sea surface temperature and productivity records for the past 240 kyr in the Arabian Sea. *Deep-Sea Research II,* **44**, 1461–1480.

SCHIEBEL, R., BIJMA, J. & HEMLEBEN, C. 1997. Population dynamics of the planktic foraminifer *Globigerina bulloides* from the eastern North Atlantic. *Deep-Sea Research,* **44**, 1701–1713.

SCHIEBEL, R., HILLER, B. & HEMLEBEN, C. 1995. Impacts of storms on recent planktic foraminiferal test production and $CaCO_3$ flux in the north Atlantic at 47°N, 20°W (JGOFS). *Marine Micropaleontology,* **26**, 115–129.

SCHULZ, H., VON RAD, U. & ITTEKKOT, V. 2002. Planktonic foraminifera, particle flux and oceanic productivity off Pakistan, NE Arabian Sea: modern analogues and application to the palaeoclimatic record. *In:* CLIFT, P.D., KROON, D., GAEDICKE, C. & CRAIG, J. (eds) *The Tectonic and Climatic Evolution of the Arabian Sea Region.* **195**, 499–516.

SPERO, H.J. & LEA, D. 1996. Experimental determination of stable isotope variability in *Globigerina bulloides*: implications for paleoceanographic reconstructions. *Marine Micropaleontology,* **28**, 231–246.

STEENS, T.N.F., GANSSEN, G. & KROON, D. 1992. Oxygen and carbon isotopes in planktic foraminifera as indicators of upwelling intensity and upwelling-induced high productivity in sediments from the north-western Arabian Sea. *In:* SUMMERHAYS, C.P., PRELL, W.C. & EMEIS, K.C. (eds) *Upwelling Systems: Evolution since the Early Miocene.* Geological Society, London, Special Publications, **64**, 107–119.

TABACHNICK, B.G. & FIDELL, L.S. 1996. *Using Multivariate Statistics.* HarperCollins, New York.

THIEDE, J. 1975. Distribution of foraminifera in surface waters of a coastal upwelling area. *Nature*, **253**, 712-714.

THUNELL, R. & REYNOLDS-SAUTTER, L. 1992. Planktonic foraminiferal faunal and stable isotopic indices of upwelling: asediment trap study in the San Pedro Basin, Southern California Bight. *In:* SUMMERHAYS, C.P., PRELL, W.C. & EMEIS, K.C. (eds) *Upwelling Systems: Evolution since the Early Miocene.* Geological Society, London, Special Publications, **64**, 77–91.

UFKES, E., JANSEN, J.H.F. & BRUMMER, G.-J.A. 1998. Living planktonic foraminifera in the eastern South

Atlantic during spring: indicators of water masses, upwelling and Congo (Zaire) River plume. *Marine Micropaleontology*, **33**, 27–53.

Van Hinte, J.E., Van Weering, T.J.C. & Troelstra, S.R. 1995. *Tracing a Seasonal Upwelling, Report on Two Cruises of RV* Tyro *to the NW Indian Ocean in 1992 and 1993*. National Museum of Natural History, Leiden.

Watkins, J.M. & Mix, A.C. 1998. Testing the effects of tropical temperature, productivity, and mixed-layer depth on foraminiferal transfer functions. *Paleoceanography*, **13**, 96–105.

Watkins, J.M., Mix, A.C. & Wilson, J. 1996. Living planktic foraminifera: tracers of circulation and productivity regimes in the central equatorial Pacific. *Deep-Sea Research II*, **43**, 1257–1282.

Watkins, J.M., Mix, A.C. & Wilson, J. 1998. Living planktic foraminifera in the central tropical Pacific Ocean: articulating the equatorial 'cold tongue' during La Niña, 1992. *Marine Micropaleontology*, **33**, 157–174.

Appendix A. *Total planktic foraminifer shell concentration >125 μm (ind. m^{-3}) and species percentage data for C1 cruise, August 1992*

Station-cast-net	Date, time (GMT +3)	Dec. longitude (°E)	Dec. latitude (°N)	Depth start (m)	Depth end (m)	T_{start} (°C)	T_{end} (°C)	Vol. filt. (m_3)	Biomass (mg m^{-3})	Tot. shell conc. (ind. m^{-3})	*B. digitata*	*D. anfracta*	*G. bulloides*	*G. falconensis*	*G. rubescens*	*G. adamsi*	*G. aequilateralis*	*G. calida*	*G. glutinata*
308-1-5	19.08.92	52.50	16.14	23	0	17.53	20.49	103	51.7	120.4	0.0	0.3	75.8	0.1	0.0	0.0	1.2	11.5	1.7
308-1-4	9:05	52.50	16.14	48	23	16.89	17.53	55	13.2	28.6	0.0	0.0	39.2	0.2	0.2	0.0	6.7	30.0	0.8
308-1-3	9:25	52.50	16.14	72	48	16.38	16.89	48	8.0	18.5	0.0	0.3	44.7	0.0	0.0	0.1	3.6	29.7	1.5
308-1-2		52.50	16.14	98	72	15.83	16.38	66	3.2	5.2	0.0	0.0	53.7	1.2	0.0	0.0	1.2	15.8	10.0
309-1-5	20.08.92	52.64	16.09	8	0	20.64	20.70	36	60.5	107.2	0.0	0.0	87.9	0.0	0.0	0.0	0.9	3.0	1.9
309-1-4	9:39	52.64	16.09	18	8	18.49	20.64	26	25.9	25.3	0.0	0.0	45.1	0.6	0.0	0.0	4.5	29.4	3.0
309-1-3	9:50	52.64	16.09	28	18	17.70	18.49	25	17.8	20.7	0.0	0.0	26.5	0.5	0.0	0.0	3.6	48.5	2.1
309-1-2		52.64	16.09	50	28	16.71	17.70	42	11.7	9.4	0.0	0.0	18.6	0.3	0.0	0.0	2.7	51.7	2.7
310-5-5	20.08.92	52.73	16.02	8	0	19.96	20.68	41	62.9	129.5	0.0	0.2	85.8	0.8	0.0	0.0	0.8	3.7	2.6
310-5-4	15:19	52.73	16.02	23	8	17.77	19.96	34	23.9	52.7	0.0	0.5	43.3	2.5	0.0	0.0	3.9	34.3	2.4
310-5-3	15:37	52.73	16.02	49	23	16.78	17.77	44	12.7	17.9	0.2	0.0	33.4	0.5	0.0	0.0	4.7	43.6	0.3
310-5-2		52.73	16.02	74	49	16.38	16.78	40	5.4	12.2	0.0	0.0	54.0	0.3	0.0	0.0	1.6	24.0	1.9
310-5-1		52.73	16.02	100	74	15.88	16.38	33	4.2	6.5	0.6	0.0	55.0	1.3	0.0	0.0	1.3	21.3	0.6
310-6-4	20.08.92	52.75	16.00	148	98	15.43	15.88	35	6.5	6.1	1.9	1.3	47.5	1.9	0.0	0.0	2.5	21.9	3.1
310-6-3	17:12	52.75	16.00	200	148	14.65	15.43	53	4.9	5.3	0.9	0.0	50.0	1.4	0.0	0.0	1.9	18.9	0.9
310-6-2	17:08	52.75	16.00	298	200	13.60	14.65	104	4.9	4.6	0.0	0.8	58.6	0.0	0.0	0.0	1.7	9.3	3.1
310-6-1		52.75	16.00	498	298	11.98	13.60	270	2.9	4.4	0.3	3.6	63.0	2.7	0.0	0.0	1.3	3.4	1.8
311-1-5	21.08.92	52.75	16.00	8	0	19.96	20.68	52	60.2	93.1	0.0	0.0	93.1	0.0	0.0	0.0	0.3	1.3	0.7
311-1-4	9:30	52.75	16.00	23	8	17.77	19.96	50	29.1	14.6	0.0	0.0	47.5	0.2	0.0	0.0	0.5	44.3	0.0
311-1-3	9:50	52.75	16.00	50	23	16.74	17.77	132	11.4	16.6	0.0	0.0	38.3	1.0	0.0	0.0	1.6	48.9	0.0
311-1-2		52.75	16.00	74	50	16.39	16.74	124	7.3	14.4	0.0	0.0	35.9	0.0	0.0	0.0	1.8	54.5	0.0
311-1-1		52.75	16.00	96	75	15.88	16.39	36	4.2	6.7	0.0	0.0	20.9	0.0	0.0	0.0	0.5	67.6	1.6
313-4-5	21.08.92	53.02	15.91	8	0	25.33	25.75	25	259.9	331.7	0.0	1.0	66.0	0.2	0.0	0.0	1.4	2.1	12.2
313-4-4	11:54	53.02	15.91	24	10	19.38	25.33	41	171.9	176.5	0.0	0.6	55.9	0.1	0.0	0.0	2.3	3.0	21.3
313-4-3	12:10	53.02	15.91	49	24	18.26	19.38	87	34.8	54.5	0.0	0.8	18.0	0.0	0.0	0.0	3.4	28.6	21.9
313-4-2		53.02	15.91	74	50	17.18	18.26	87	18.8	63.3	0.0	0.8	46.0	0.0	0.0	0.0	0.9	11.7	11.1
313-4-1		53.02	15.91	100	75	16.52	17.18	60	9.3	46.8	0.0	0.3	55.7	0.2	0.0	0.0	0.7	8.3	7.4
313-dc-4	22.08.92	52.94	15.88	148	99	15.37	16.52	94	6.2	33.7	0.0	2.5	55.6	0.3	0.0	0.0	0.5	2.5	14.5
313-dc-3	12:45	52.94	15.88	196	150	14.45	15.37	98	9.8	52.8	0.0	2.1	58.7	0.4	0.0	0.0	0.9	2.7	17.7
313-dc-2	13:49	52.94	15.88	300	199	13.42	14.45	278	14.2	37.3	0.0	3.7	48.8	1.3	0.0	0.0	1.6	2.5	17.0
313-dc-1		52.94	15.88	498	300	11.75	13.42	478	10.9	58.7	0.0	1.5	55.9	0.3	0.0	0.0	0.6	0.8	13.7

G. uvula	*G. conglobatus*	*G. ruber*	*G. tenellus*	*G. sacculifer* (−)	*G. sacculifer* (+)	*G. menardii*	*G. scitula*	*G. theyeri*	*G. tumida*	*G. hexagona*	*H. parapelagica*	*N. dutertrei*	*N. pach (sin)*	*O. universa*	*P. obliquiloculata*	*T. iota*	*T. humillis*	*T. quinqueloba*	Aberrant	P.F. indet.
0.3	0.0	0.1	0.0	0.0	0.0	3.3	0.0	0.0	0.0	0.0	0.2	2.6	0.0	0.0	0.0	1.0	0.0	0.3	0.3	1.3
0.2	0.0	0.0	0.0	0.0	0.0	8.4	0.0	0.0	0.0	0.0	1.8	2.5	0.0	0.0	0.0	7.0	0.0	0.8	1.1	1.1
0.3	0.0	0.1	0.1	0.0	0.0	4.0	0.4	0.0	0.0	0.0	1.2	1.5	0.0	0.0	0.0	1.2	0.0	9.9	0.7	0.4
0.4	0.0	3.9	0.0	0.0	0.0	4.6	1.5	0.0	0.0	0.8	0.8	2.3	0.0	0.0	0.0	0.4	0.0	2.3	0.4	0.8
0.3	0.0	0.0	0.0	0.0	0.0	0.2	0.0	0.0	0.0	0.0	0.0	2.4	0.0	0.0	0.0	0.0	0.0	2.8	0.7	0.0
0.0	0.0	0.4	0.4	0.2	0.0	4.5	0.0	0.0	0.0	0.0	1.4	4.7	0.2	0.0	0.0	4.0	0.0	1.0	0.4	0.2
0.5	0.0	0.0	0.0	0.3	0.0	6.4	0.3	0.0	0.0	0.0	3.1	3.6	0.0	0.0	0.0	2.8	0.0	1.5	0.0	0.3
0.0	0.0	0.7	0.3	0.3	0.0	16.2	0.0	0.0	0.0	0.3	1.4	2.7	0.3	0.0	0.0	0.0	0.0	1.4	0.0	0.3
0.0	0.0	0.0	0.4	0.0	0.0	1.1	0.0	0.0	0.0	0.0	0.1	2.9	0.0	0.0	0.0	0.4	0.0	1.0	0.0	0.2
0.0	0.0	0.0	0.0	0.0	0.0	4.6	0.0	0.0	0.0	0.0	1.6	3.6	0.1	0.0	0.1	1.3	0.0	1.0	0.4	0.5
0.0	0.0	0.0	0.0	0.0	0.0	4.9	0.3	0.0	0.0	0.0	3.0	2.4	0.2	0.0	0.0	2.7	0.0	2.9	0.5	0.3
0.0	0.0	0.5	0.0	0.0	0.0	12.3	0.5	0.0	0.0	0.0	0.3	1.4	0.3	0.0	0.0	0.0	0.0	2.5	0.5	0.0
0.0	0.0	0.6	0.6	0.0	0.0	8.8	0.0	0.0	0.0	0.0	4.4	1.3	1.3	0.0	0.0	1.3	0.0	1.3	0.0	0.6
0.0	0.0	0.6	0.0	0.6	0.0	5.6	0.0	0.6	0.0	0.6	3.8	4.4	0.0	0.0	0.0	0.0	0.0	3.1	0.0	0.6
0.0	0.0	0.9	0.5	0.0	0.0	6.6	0.0	1.4	0.0	0.9	1.9	3.8	0.9	0.0	0.0	0.0	0.0	9.0	0.0	0.0
0.0	0.0	0.8	0.0	0.0	0.0	10.1	0.0	0.6	0.0	2.8	0.3	3.1	1.4	0.0	0.3	0.0	0.0	5.6	0.3	1.1
0.0	0.0	1.1	0.4	0.2	0.0	7.0	0.4	0.0	0.0	3.4	0.7	4.2	1.6	0.0	0.0	0.9	0.0	2.9	0.1	0.9
0.2	0.0	0.2	0.2	0.3	0.0	0.2	0.0	0.0	0.0	0.0	0.0	1.0	0.0	0.0	0.0	0.0	0.0	2.6	0.0	0.0
0.0	0.0	0.0	0.0	0.0	0.0	0.2	0.0	0.0	0.0	0.0	2.4	1.1	0.0	0.0	0.0	0.4	0.0	1.8	0.9	0.7
0.0	0.0	0.0	0.0	0.0	0.0	0.0	0.0	0.2	0.0	0.0	2.7	1.2	0.0	0.0	0.0	0.0	0.0	3.9	0.4	1.9
0.1	0.0	0.1	0.0	0.0	0.0	0.4	0.0	0.0	0.0	0.0	1.1	0.6	0.0	0.0	0.0	0.7	0.0	2.7	0.4	1.5
0.0	0.0	1.1	0.0	0.0	0.0	2.2	0.0	0.0	0.0	0.0	1.1	3.3	0.0	0.0	0.0	0.0	0.0	0.5	0.0	1.1
0.6	0.0	6.3	1.0	0.8	0.0	0.6	0.0	0.0	0.0	0.0	0.0	5.3	0.2	0.0	0.0	0.2	0.0	0.0	1.6	0.6
0.0	0.0	5.3	1.5	1.8	0.0	0.6	0.0	0.0	0.0	0.0	0.4	5.2	0.1	0.0	0.2	0.6	0.0	0.4	0.5	0.3
0.1	0.0	3.7	2.4	1.9	0.1	3.1	0.0	0.0	0.0	0.0	2.6	10.1	0.0	0.1	0.0	1.0	0.0	1.1	0.1	1.0
0.2	0.0	3.9	0.6	0.6	0.0	4.3	0.8	0.0	0.0	0.0	0.8	4.0	2.3	0.0	0.2	0.4	0.0	7.6	1.6	2.4
1.0	0.0	2.7	0.6	0.3	0.0	11.5	0.8	0.0	0.0	0.1	0.6	2.1	2.2	0.0	0.1	0.3	0.0	2.4	1.1	1.7
0.0	0.0	1.7	0.5	0.4	0.0	6.8	1.6	0.4	0.0	0.9	1.3	1.4	5.9	0.0	0.0	0.1	0.0	2.0	0.3	0.7
0.1	0.0	1.3	0.6	0.2	0.0	3.1	0.6	0.1	0.0	0.0	1.6	1.7	5.2	0.0	0.2	0.2	0.0	2.4	0.1	0.5
0.2	0.0	1.4	0.8	0.1	0.0	1.6	0.6	0.1	0.0	0.4	1.1	1.1	8.7	0.0	0.0	0.0	0.0	8.1	0.0	0.9
0.3	0.0	1.2	0.8	0.2	0.0	1.6	0.2	0.2	0.0	1.0	0.0	1.3	11.7	0.0	0.3	0.3	0.0	6.5	0.2	1.4

Appendix B. *Planktic foraminifer shell concentration >125 μm (ind. m^{-3}) and species percentage data for C2 cruise, August 1992*

Station-cast-et	Date, time (GMT +3)	Dec. longitude (°E)	Dec. latitude (°N)	Depth start (m)	Depth end (m)	T_{start} (°C)	T_{end} (°C)	Vol. filt. (m$_3$)	Biomass (mg m^{-3})	Tot. shell conc. (ind. m^{-3})	*B. digitata*	*D. anfracta*	*G. bulloides*	*G. falconensis*	*G. rubescens*	*G. adamsi*	*G. aequilateralis*	*G. calida*	*G. glutinata*
917-2-5	25.02.93	52.92	15.90	12	0	25.71	25.80	21	40.7	19.2	0.0	0.0	1.0	0.7	0.0	0.0	20.8	3.0	8.6
917-2-4	8:50	52.92	15.90	27	12	24.89	25.71	22	66.2	17.5	0.0	0.0	2.8	0.7	0.0	0.0	12.2	14.6	4.2
917-2-3	9:15	52.92	15.90	52	27	24.32	24.89	43	80.8	49.1	0.0	0.0	6.8	1.1	0.0	0.0	17.0	7.3	13.8
917-2-2		52.92	15.90	78	52	23.09	24.32	79	19.6	17.1	0.0	0.2	6.3	9.6	0.0	0.0	8.6	12.5	10.8
917-2-1		52.92	15.90	102	78	19.96	23.09	68	12.1	16.7	0.0	0.1	2.7	6.4	0.0	0.0	9.4	19.5	5.9
917-1-4	25.02.93	52.97	15.89	153	101	16.26	19.96	75	10.1	8.0	0.0	0.7	6.4	4.2	0.0	0.0	6.4	41.3	8.4
917-1-3	7:23	52.97	15.89	203	153	15.67	16.26	75	10.7	12.5	2.2	0.0	8.7	7.4	0.2	0.0	4.2	22.4	13.7
917-1-2	8:15	52.97	15.89	302	203	13.75	15.67	184	2.8	3.8	0.6	0.2	3.6	26.0	0.0	0.0	5.6	20.9	11.9
917-1-1		52.97	15.89	502	302	11.88	13.75	240	6.6	7.7	1.2	0.6	5.1	15.1	0.0	0.0	6.5	10.3	18.9
918-2-5	26.02.93	52.84	15.96	12	0	25.86	25.95	35	43.2	25.3	0.0	0.0	1.2	0.2	0.0	0.0	20.8	0.2	8.6
918-2-4	7:05	52.84	15.96	27	12	25.22	25.86	47	71.1	21.9	0.0	0.0	0.6	0.0	0.0	0.0	26.7	0.7	10.9
918-2-3	8:30	52.84	15.96	52	27	24.60	25.22	97	76.1	26.5	0.0	0.0	3.4	0.5	0.0	0.0	29.6	10.3	14.1
918-2-2		52.84	15.96	78	52	22.56	24.60	132	23.9	11.6	0.0	0.0	5.5	1.2	0.0	0.0	45.1	15.8	8.8
918-2-1		52.84	15.96	103	78	19.25	22.56	101	14.1	11.5	0.0	0.0	7.2	3.4	0.0	0.0	17.4	17.5	7.0
919-1-5	26.02.93	52.73	16.00	10	0	25.76	25.90	12	61.0	32.6	0.0	0.0	2.0	0.0	0.0	0.0	16.7	1.4	12.3
919-1-4	16:47	52.73	16.00	26	10	25.59	25.76	19	22.3	24.1	0.0	0.0	2.6	0.3	0.0	0.0	19.2	1.2	12.8
919-1-3	—	52.73	16.00	52	26	24.36	25.59	50	89.4	55.4	0.0	0.0	5.9	0.6	0.0	0.0	23.7	4.4	11.2
919-1-2		52.73	16.00	77	52	23.52	24.36	91	23.6	21.6	0.0	0.0	7.8	1.8	0.0	0.0	35.5	13.5	11.7
919-1-1		52.73	16.00	102	77	19.40	23.52	70	9.5	12.3	0.0	0.2	7.3	4.0	0.0	0.0	22.6	20.5	6.2
920-2-5		52.64	16.08	11	0	25.52	25.52	16	54.0	75.2	0.0	0.0	2.4	0.0	0.0	0.0	22.0	4.1	11.5
920-2-4	27.02.93	52.64	16.08	27	11	25.49	25.52	46	36.3	27.9	0.0	0.0	1.6	0.0	0.0	0.0	23.0	4.5	9.8
920-2-3	8:45	52.64	16.08	53	27	24.60	25.49	79	52.1	34.6	0.0	0.2	2.1	0.6	0.0	0.0	29.1	6.4	12.1
920-2-2	9:15	52.64	16.08	78	53	23.11	24.60	135	15.9	10.4	0.0	0.4	6.3	0.9	0.2	0.0	23.1	20.5	8.2
920-2-1		52.64	16.08	102	78	19.93	23.11	105	12.2	7.0	0.0	0.0	2.5	1.0	0.0	0.0	14.0	30.0	8.9
920-1-4	27.02.93	52.70	16.09	153	103	17.48	19.93	168	7.0	5.7	0.0	0.0	4.3	0.4	0.0	0.0	12.4	49.4	10.7
920-1-3	7:15	52.70	16.09	202	153	16.53	17.48	146	7.7	5.6	0.0	0.2	2.9	1.4	0.0	0.0	9.2	42.9	10.4
920-1-2	8:15	52.70	16.09	303	202	13.98	16.53	269	27.9	4.0	1.3	0.9	4.4	1.9	0.0	0.0	10.9	22.7	10.0
920-1-1		52.70	16.09	501	303	12.56	13.98	282	15.1	6.1	11.7	0.6	4.3	3.3	0.0	0.0	5.6	10.0	12.9
922-2-5		52.52	16.17	12	0	25.54	25.55	48	77.2	85.0	0.0	0.0	4.9	0.4	0.0	0.0	3.9	3.1	14.5
922-2-4	27.02.93	52.52	16.17	26	12	25.53	25.54	58	67.2	59.5	0.0	0.0	4.8	0.2	0.0	0.0	3.6	2.8	15.8
922-2-3	7:00	52.52	16.17	52	26	24.56	25.53	106	45.7	33.1	0.0	0.2	6.8	1.0	0.0	0.0	9.1	12.0	16.7
922-2-2	—	52.52	16.17	77	52	23.75	24.56	149	16.3	9.5	0.0	0.0	5.3	4.8	0.0	0.1	11.1	19.0	12.6
922-2-1		52.52	16.17	102	77	21.00	23.75	169	4.7	2.9	0.0	0.0	7.2	6.4	0.0	0.0	11.8	24.1	8.3

G. uvula	*G. conglobatus*	*G. ruber*	*G. tenellus*	*G. sacculifer (−)*	*G. sacculifer (+)*	*G. menardii*	*G. scitula*	*G. theyeri*	*G. tumida*	*G. hexagona*	*H. parapelagica*	*N. dutertrei*	*N. pach (sin)*	*O. universa*	*P. obliquiloculata*	*T. iota*	*T. humillis*	*T. quinqueloba*	Aberrant	P.F. indet.
0.0	0.0	13.5	3.0	44.2	0.0	1.0	0.0	0.0	0.0	0.0	0.0	2.0	0.0	0.3	0.0	0.0	0.0	0.0	0.0	2.0
0.0	0.0	14.6	3.5	44.8	0.0	0.0	0.0	0.0	0.0	0.0	0.7	0.7	0.0	0.3	0.0	0.0	0.0	0.0	0.7	0.3
0.0	0.0	32.6	6.7	9.4	0.4	0.2	0.0	0.0	0.0	0.0	0.0	3.2	0.0	0.4	0.1	0.0	0.0	0.0	0.0	1.1
0.2	0.0	30.4	14.2	3.0	0.2	0.0	0.0	0.0	0.0	0.0	0.0	1.0	0.0	0.7	0.0	0.0	0.0	0.0	0.2	2.2
0.0	0.0	34.9	16.1	0.1	0.0	0.0	0.1	0.1	0.0	0.6	0.0	0.6	0.0	0.0	0.0	0.0	0.1	0.0	1.5	1.9
0.0	0.0	19.1	6.0	2.0	0.0	0.0	0.0	0.0	0.0	0.2	2.4	0.7	0.0	0.7	0.2	0.0	0.0	0.0	0.4	0.7
0.0	0.0	22.6	12.5	1.0	0.1	0.0	0.0	0.0	0.0	1.3	1.1	0.3	0.0	0.0	0.4	0.0	0.0	0.0	0.2	1.5
0.0	0.0	18.6	5.8	2.3	0.0	0.0	0.0	0.0	0.0	0.0	1.3	0.8	0.0	0.0	0.2	0.0	0.0	0.2	0.2	1.9
0.0	0.0	18.4	11.8	0.7	0.0	0.1	0.2	0.0	0.0	9.1	0.3	0.0	0.0	0.1	0.0	0.0	0.0	0.0	0.1	1.4
0.0	0.0	27.5	6.6	30.8	0.2	0.6	0.0	0.0	0.0	0.0	0.0	2.1	0.0	0.6	0.0	0.0	0.0	0.0	0.0	0.6
0.0	0.0	20.3	5.0	32.2	0.1	1.0	0.0	0.0	0.0	0.0	0.0	1.7	0.0	0.4	0.0	0.0	0.0	0.0	0.0	0.3
0.0	0.0	22.3	6.2	9.2	0.4	0.1	0.0	0.0	0.0	0.1	0.0	2.5	0.0	0.8	0.0	0.0	0.0	0.0	0.2	0.4
0.1	0.0	13.6	3.6	3.4	0.0	0.0	0.0	0.0	0.0	0.0	0.5	1.3	0.0	0.4	0.1	0.0	0.0	0.0	0.0	0.6
0.3	0.0	27.2	13.7	2.5	0.1	0.1	0.0	0.1	0.0	0.3	0.7	1.3	0.0	0.2	0.0	0.0	0.0	0.2	0.0	0.7
0.0	0.0	35.2	4.1	24.9	0.0	0.7	0.0	0.0	0.0	0.0	0.0	1.0	0.0	0.3	0.0	0.0	0.0	0.0	0.0	1.4
0.0	0.0	34.7	4.1	20.4	0.0	0.9	0.0	0.0	0.0	0.0	0.0	2.0	0.0	0.3	0.0	0.0	0.0	0.0	0.0	1.5
0.0	0.0	28.3	6.4	14.4	0.3	0.4	0.0	0.0	0.0	0.0	0.0	2.7	0.0	0.7	0.0	0.0	0.0	0.0	0.0	1.0
0.1	0.0	17.2	2.9	3.7	0.6	0.0	0.0	0.0	0.0	0.0	0.0	1.9	0.0	1.2	0.1	0.1	0.0	0.1	0.1	1.6
0.0	0.0	22.5	3.7	6.0	0.5	0.0	0.2	0.0	0.0	0.3	0.0	1.9	0.0	1.1	0.2	0.0	0.0	0.2	0.0	2.8
0.0	0.2	22.6	5.8	19.6	0.1	4.5	0.0	0.0	0.0	0.0	1.1	4.0	0.0	0.2	0.0	0.0	0.0	0.0	0.0	1.8
0.0	0.0	20.5	7.1	20.2	0.0	7.8	0.0	0.0	0.0	0.0	0.0	4.3	0.0	0.6	0.3	0.0	0.0	0.0	0.2	0.2
0.0	0.0	20.2	7.7	11.9	0.2	5.0	0.0	0.0	0.0	0.0	0.2	2.9	0.0	0.5	0.0	0.0	0.0	0.0	0.0	0.6
0.0	0.0	16.8	10.4	4.5	0.7	1.6	0.0	0.0	0.0	0.0	0.6	1.2	0.5	0.6	0.4	0.2	0.0	1.3	0.1	1.5
0.0	0.0	14.1	21.0	2.7	0.2	1.1	0.2	0.0	0.0	0.4	1.3	0.7	0.2	0.0	0.2	0.0	0.0	0.0	0.4	1.1
0.0	0.0	9.1	1.8	2.4	0.0	0.4	0.6	0.3	0.0	0.1	4.2	1.3	0.0	0.6	0.3	0.0	0.0	0.0	0.1	1.7
0.2	0.0	13.2	4.4	4.9	0.0	0.2	0.5	0.4	0.0	0.2	6.6	0.6	0.2	0.2	0.0	0.3	0.0	0.2	0.0	1.0
1.5	0.0	17.4	13.8	4.7	0.6	0.4	0.4	0.8	0.0	2.6	2.2	1.4	0.0	0.3	0.0	0.2	0.2	0.2	0.3	1.0
0.0	0.0	19.4	14.2	1.8	0.0	0.0	0.8	0.0	0.0	12.7	0.5	0.4	0.0	0.0	0.0	0.0	0.0	0.2	0.1	1.3
0.0	0.0	36.4	7.7	22.3	0.1	1.4	0.0	0.0	0.0	0.0	0.0	4.2	0.0	0.1	0.0	0.0	0.0	0.0	0.1	0.8
0.0	0.0	38.1	4.0	24.6	0.0	1.8	0.0	0.0	0.0	0.0	0.0	3.3	0.0	0.2	0.1	0.0	0.0	0.0	0.3	0.5
0.0	0.0	25.4	6.3	13.3	0.1	3.3	0.0	0.0	0.0	0.0	0.0	3.5	0.0	0.2	0.2	0.0	0.0	0.0	0.0	2.0
0.0	0.0	17.7	16.0	6.9	0.0	1.5	0.0	0.0	0.0	0.2	0.0	2.0	0.0	0.0	0.0	0.0	0.0	0.0	0.4	2.3
0.0	0.0	23.3	6.2	5.9	0.0	1.3	0.0	0.0	0.0	0.3	0.0	2.7	0.0	0.3	0.3	0.0	0.0	0.0	0.3	1.6